Seasonal, landscape-scale variation in bacterial and fungal communities

By

Paige Hansen

Submitted to the graduate degree program in Ecology and Evolutionary Biology and the Graduate Faculty of the University of Kansas in partial fulfillment of the requirements for the degree of Master of Arts.

Chair: Benjamin Sikes

Sharon Billings

Maggie Wagner

Jorge Soberon

Date Defended: 30 October 2020

The thesis committee for Paige Hansen certifies that this is the
approved version of the following thesis:

Seasonal, landscape-scale variation in bacterial and fungal communities

Chair: Benjamin Sikes

Date Approved: 30 October 2020

Abstract

Soil bacterial and fungal communities change dramatically over seasons and across multiple climate and environmental gradients. Little work has tested if the impact of these gradients on soil communities depends on the season in which they are measured, or whether seasonal community dynamics differ predictably across gradients. Given close links between microbial community variation and microbial function, more knowledge of community changes across these gradients in a single season and across the growing season could allow for a better understanding of microbial function at the landscape scale. We used amplicon sequencing to determine how the diversity and structure of soil bacterial and fungal communities respond to broad differences in environment, including historical precipitation, land use, and soil depth. We examined communities in spring and fall separately, then assessed whether community change across seasons depended on these same factors. We found that within-season variation in bacterial and fungal communities responded similarly to precipitation, land use, and depth. In spring and fall, these factors had similar impacts on bacterial and fungal communities, with depth explaining the majority of variation in diversity and community structure. Strong shifts in diversity and community structure across seasons were observed only at the 0-5 cm depth, and differed solely based on annual precipitation (not land use). While soil depth plays an important role in structuring microbial communities in both seasons, our results indicate that across seasons, only microbial communities at the soil's surface are sensitive to climate differences. Key edaphic variables that change with soil depth and precipitation (i.e., soil moisture, pH, and organic carbon content) may simultaneously predict landscape-scale community variation within and across seasons. As patterns of microbial function in individual seasons and across seasons may respond differently to environmental gradients, future work determining if community structure and function are equally

linked across environmental gradients and seasons will be key to assessments of functional redundancy, and to better predict change in ecosystem function.

Acknowledgments

This thesis would not have been possible without the help and support of many people. First and foremost, I give sincere gratitude to my undergraduate and graduate advisor, Dr. Ben Sikes. Thank you so much for teaching me how to get excited about my research, for encouraging me to pursue all my goals to the fullest extent, and for always believing in my ability as a scientist.

I would also like to thank my committee members, Drs. Sharon Billings, Maggie Wagner, and Jorge Soberon, for their excellent advice on this project. This thesis would not have been possible without your help.

As this work represents a portion of a larger, multi-institutional project, I have many people across the state of Kansas to acknowledge for their involvement in my research. I would like to thank the many technicians, undergraduate students, and graduate students in the labs of Drs. Jim Bever, Sharon Billings, Matt Kirk, Terry Loecke, Ari Jumponnen, Tom Platt, Greg Houseman, and Chuck Rice for their help in collecting, homogenizing, and organizing soil samples. Thank you to Dr. Tanya Semenova-Nelsen for her advice on DNA extraction protocols, and to Austin Yoder for his help in generating bacterial sequencing libraries. Many thanks to Dr. Maggie Wagner for her help in developing creative statistical methods to analyze my data, and to Dr. Jim Bever for his help in developing linear models that I could use in doing so. Sincere thanks to Theo Michaels, who dedicated substantial time to reviewing, editing, and commenting on many thesis drafts. I truly appreciate the time each of you has dedicated to my scientific success.

Outside of this thesis, I had the wonderful opportunity to spend a summer conducting research at Leiden University, Netherlands. I want to give special thanks to Dr. Tanya Semenova-Nelsen for her help in making this experience possible, as well as for her advice in securing Swedish PhD offer. Though a broken elbow and COVID-19 shutdowns prevented me from participating in these experiences to the fullest extent, I made many friends, learned a lot about science, and most importantly, had fun.

I am fortunate to have made many friends during my time at KU, and I would not have come this far without their support. In no particular order, to Ali, Theo, Amanda, Antoine, Andy, Haley, Lígia, and all my friends at KU and beyond, thank you for always making me laugh, and for helping me become a more well-rounded person and scientist. I will always be grateful for each of your friendships.

I am also fortunate to have the love and support of my family. To my parents, thank you for being my biggest cheerleaders, as you always have been and always will be. To my brother Jack, my cousins Grace and Meredith, and my grandparents, thank you for finding small ways to make me smile each week. I greatly appreciate all the ways you have supported me through the many ups and downs of graduate school.

Lastly, I want to acknowledge those who funded my graduate work. While this project was supported by a National Science Foundation Established Program to Stimulate Competitive Research (EPSCoR) Research Infrastructure Improvement Program Track-1 Award (OIA-1656006, NSF-0079054), I was personally supported by a Madison and Lila Self Graduating Senior Fellowship, an Ida H. Hyde Scholarship for Women in Science to Study at a Non-KU Institution, and a KU General Research Fund (GRF). I would like to acknowledge Drs. John Kelly and Ben Sikes for administering the latter funding, which helped keep me employed as a student as I finished the last portions of my thesis. None of my work would have been possible without this financial support.

I dedicate this thesis to the many conversations I have had about place, and what it means to conduct research on land marred by a long history of violence. The land in Kansas has been

stolen, colonized, fought over, and bled on, nearly entirely at the expense of indigenous Americans and Black people. These legacies of violence are intimately woven into the ecosystems we claim to rescue, rehabilitate, and preserve. As such, our past and future actions deeply intertwined with our science. Disregarding these legacies from ecological work is a disservice to our ecosystems and to humanity's collective history.

Table of Contents

1 Introduction

Soil bacterial and fungal communities often shift dramatically in structure and diversity from season to season. These dynamics are influenced by many environmental factors that also shift with season, including precipitation, temperature, plant community composition and biomass, and edaphic properties, including soil moisture and nutrient availability (Bardgett et al., 1999; Habekost et al., 2008; Shigyo et al., 2019). Combined, these factors generate seasonal changes in microbial communities that can be as great as shifts across vast spatial distances (i.e., ~4000 km; Averill et al., 2019; Lauber et al., 2013), but are generally consistent within a given season from year to year (Cruz-Martínez et al., 2009). The scale of these differences suggests that the season in which communities are measured matters greatly to assessments of microbial response to environmental change, as any community shifts must be gauged against their underlying seasonal dynamics. Although rarely explicitly addressed, this variation is often avoided by methods that try to consistently sample at the same time of year (e.g., peak biomass). This means our current understanding of how bacterial and fungal communities change in response to environmental perturbations is often viewed through a static, rather than seasonal lens.

While microbial communities shift seasonally, little work has explored whether the magnitudes of these shifts differ along climate gradients. Because bacterial and fungal community response to current environmental perturbations is often contingent on historical conditions (Hawkes and Keitt, 2015), it is likely that magnitudes of seasonal community change are reflective of a community's historical climate. Among the many climate factors, including temperature, we choose to focus specifically on precipitation. Multiple studies have shown that historical precipitation plays a significant role in structuring bacterial and fungal communities (Averill et al., 2016; Hawkes et al., 2017, 2011; Waring and Hawkes, 2018). Resilience to precipitation changes may also depend on historical conditions; communities from sites with historically more variable climates tend to be more resistant to fluctuations in precipitation than communities from historically stable climates (Evans and Wallenstein, 2012). As such, in addition to structuring bacterial and fungal communities within a single season, it is possible that historical precipitation influences magnitudes of seasonal community shifts, especially those driven by seasonal rainfall fluctuations.

Historical land use may also drive environmental shifts that alter magnitudes of seasonal community change. When measured at a single time point, land use history often drives significant microbial community variation (Bissett et al., 2011; Brinkmann et al., 2019; Jangid et al., 2011; Turley et al., n.d.; Xiang et al., 2014), with agricultural (or heavily-modified) lands usually harboring soil microbial communities that are distinct from those in native systems. This variation is often linked to differences in plant root abundance (Broeckling et al., 2008), soil structure (Smith et al., 2014), and nutrient availability (Xiang et al., 2014) among land use types. Because environmental variables like these vary predictably with broad land use categories (e.g., agricultural vs undisturbed), different land use types provide a general framework to broadly test hypotheses about the impacts of these variables on seasonal microbial community change. For example, rooting depth and abundance differ with land use history (Billings et al., 2019). These differences could drive microbial community variation among land uses by changing the availability of root habitats and root exudates. Given seasonal plant growth and changes in the quantity and timing of root exudates with seasonal changes in aboveground conditions (Canarini et al., 2019), seasonal community shifts might be greatest in native systems, where more roots are present. Similarly, seasonal management practices like fertilization create differences in mineral nutrient availability among land uses that vary throughout the year (Ge et al., 2009). Strong competitive interactions in microbial communities when and where nutrients are less readily available (e.g., native systems) could generate greater community fluctuations compared to soils with high mineral nutrient content (e.g., agricultural systems).

The effects of precipitation and land use on seasonal community changes may differ as one moves from shallow to deep soils. Specifically, rainfall influences vertical water fluxes (Kurc and Small, 2007; Weiler and Naef, 2003), and specific land uses like conventional agriculture change soil structure and nutrient availability (Veenstra and Lee Burras, 2015) in ways that may have varying effects on communities at different soil depths. In combination with strong shifts in microbial communities across soil depths (Feng et al., 2019; Jumpponen et al., 2010; Will et al., 2010), the effects of historical precipitation and land use could generate communities that are unique to precipitation and land use throughout the profile. It is likely that the effects of these factors will be most pronounced in communities at the soil's surface. Here, microbial communities are more exposed and sensitive to seasonal environmental perturbations (Griffiths et al., 2003). As such, surficial communities are likely to experience greater magnitudes of seasonal change than communities in deep soil across gradients of both precipitation and land use. As microbial community variation is closely linked with microbial function (Philippot et al., 2013; Strickland et al., 2009), more concise knowledge of community variation across overlaid climate (i.e., precipitation) and environmental (i.e., land use and soil depth) gradients, both within a single season and across the growing season, could allow for a better understanding of microbial function at the landscape scale.

To determine landscape-scale variation in soil microbial communities, both within and across seasons, we first assessed how historical precipitation, land use, and soil depth shape communities immediately before and after the growing season. We determined how these factors impact the diversity and community structure of both bacteria and fungi. After assessing within-season community variation, we examined the extent to which magnitudes of seasonal community shifts depend on precipitation, land use, and soil depth. We aimed to use these broad climate and environmental categories to predict the fundamental variables most strongly contributing to microbial community variation within and across seasons. To do so, we collected replicate soil samples in spring and fall 2018 throughout the state of Kansas. These samples are representative of a strong annual precipitation gradient, three distinct land uses (native prairies, restored prairies, and agricultural fields), and five depth increments to 150 cm (Figure 1). With these soils, we used amplicon sequencing (Illumina MiSeq) to characterize bacterial (16S) and fungal (ITS2) communities, and assess their static and seasonal responses to our climate and environmental categories.

In both spring and fall, we predicted that historical precipitation, land use, and soil depth would all contribute to variation in bacterial and fungal communities. Specifically, we hypothesized that changes in edaphic properties throughout the soil profile would create differences in microbial communities that were greatest between surficial and deep soils. In comparing communities across the precipitation gradient, we predicted that communities from the historically driest and wettest regions would be most distinct. Land use would also shape bacterial and fungal communities, with those in agricultural and native systems being most dissimilar. When comparing magnitudes of seasonal change, we predicted that seasonal community changes would be more muted in dry than in wet regions. Additionally, because bacteria are more sensitive to drought and desiccation than fungi (Barnard et al., 2013; de Vries et al., 2018), bacterial communities may experience greater magnitudes of seasonal change than fungi overall. We had competing hypotheses for seasonal differences with land use. In native prairies, competitive interactions among microbes where there are greater roots and fewer available nutrients may drive larger seasonal changes than in croplands. However, the seasonal nature of annual agriculture (e.g. tillage, planting, harvest) may also produce more dramatic seasonal shifts in communities compared to restored or undisturbed grasslands (Lauber et al., 2013). Lastly, because soil depth can determine the exposure of microbial communities to precipitation and land use effects, we predicted that depth would likely play a key role in shaping seasonal community shifts related to precipitation and land use.

2 Materials and Methods

2.1 Site selection and experimental design

We chose to conduct our study in the state of Kansas because it is a landscape-scale ‘lab’ for studies on variations in precipitation and land use history. Kansas is characterized by a precipitation gradient that ranges from 350 mm per year in the West to 1162 mm per year in the East (Figure 1A). The state is also comprised of a patchwork of land uses, including remnant, unplowed tall- and mixed grass prairies, active crop lands, and abandoned agricultural fields, some of which are now active restorations. We took advantage of Kansas’s precipitation gradient and these variable land use histories to assess how they and soil depth impact magnitudes of seasonal change in bacterial and fungal communities. We selected regions whose historical precipitation regime represents relatively dry (West, 533 mm/y), intermediate (Central, 865 mm/y), and wet (East, 1045 mm/y) amounts of annual precipitation (Figure 1A). While the timing of seasonal rainfall events differs among these regions, precipitation is greater in the spring than in the fall in all three (Figure S1). In each region, we located sites at research facilities representing three land use histories: a remnant native grassland, a post-agricultural restoration, and an active agricultural field (Figure 1B). Because relatively little land in Kansas represents remnant grassland, these land use histories are pseudoreplicated within precipitation region; to maintain consistency with availability of remnant prairie, we sampled from only one replicate of each land use type in each precipitation region. While broad, these three land use categories encapsulate expected variation in land management and crops, as well as in soil property variables and root abundance. For example, all three restorations (West, Central, and East), were seeded with native forbs and grasses, but vary in management (e.g., mowing, burning) and in restoration age. Likewise, while all sampled agricultural fields are regularly tilled and planted with cover crops, they are rarely planted at the same time and with the same crops, including the year we sampled. Information about individual site location, land use history, annual precipitation, soil type, and plant community at time of sampling is located in Table 1. At each site, we established four plots to sample soils.

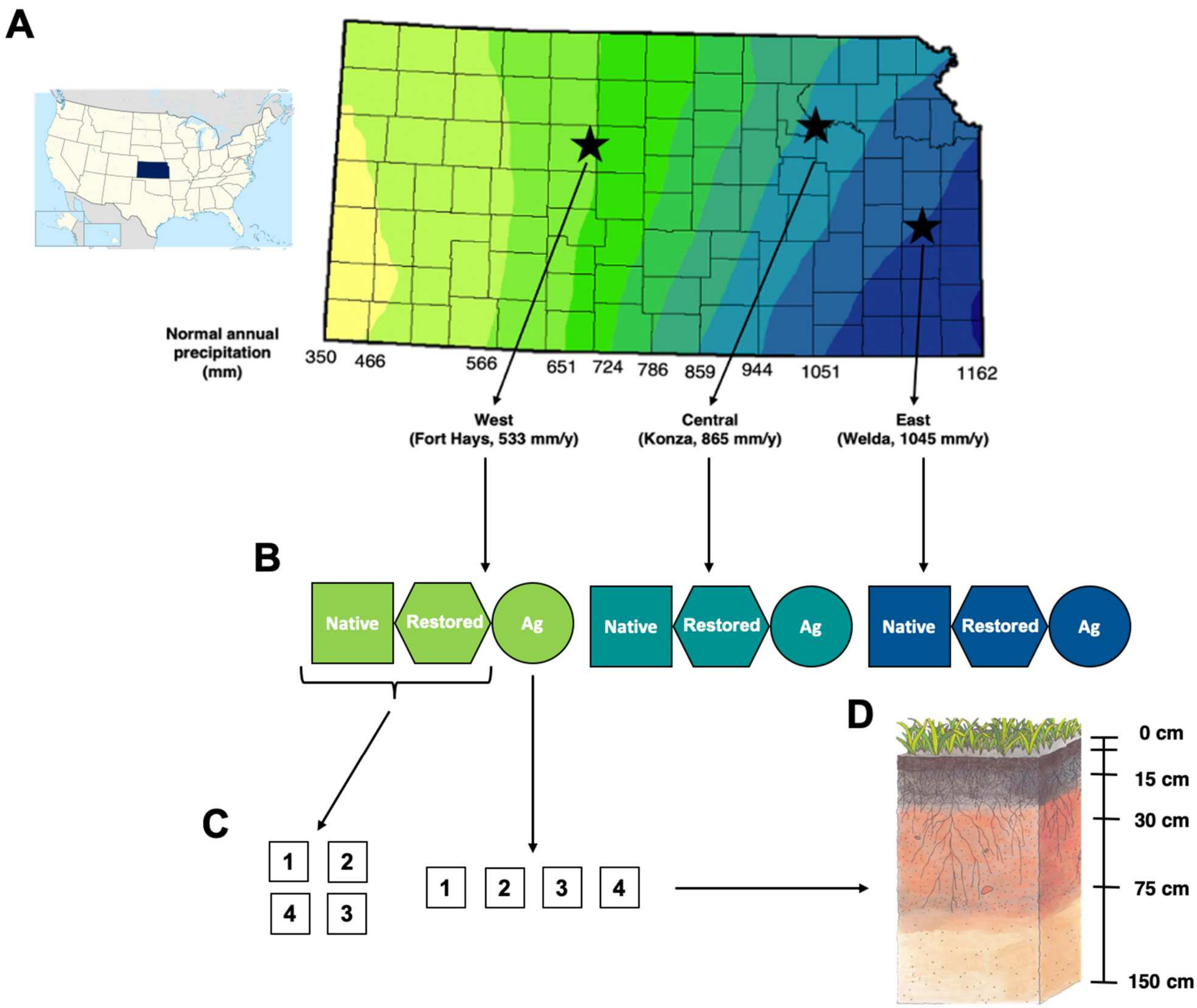

Figure 1. Complete sampling design. **(A)** Kansas's location in the United States, and the state's normal annual precipitation from 1981-2010. Lighter and darker colors represent lower and higher amounts of annual precipitation, respectively. Yearly precipitation estimates in mm are indicated along the bottom of the map. Stars represent sites selected for sampling. **(B)** In each precipitation region, we sampled from a native prairie, a restored prairie, and an agricultural field. **(C)** We sampled from 4 plots in each land use history. Native and restored plots were arranged quadratically, and agricultural plots were arranged linearly. **(D)** In each plot, 3 replicate soil cores were taken to a maximum depth of 150 cm, and divided into 0-5 cm, 5-15 cm, 15-30 cm, 30-75 cm, and 75+ cm increments. The 3 replicates from each plot were combined to create 1 single sample per plot. Figure adapted from Wikipedia Commons, the Kansas Office of the State Climatologist, and the USDA-NRCS.

Table 1. Names, climatic regions, land use histories, exact locations, and environmental characteristics of all sampled sites.

Location name	Precipitation region	Land use history	Latitude, longitude	Annual precipitation (mm/y)	Soil type	Plant community
Hays Experimental Range	West	Native prairie	38.84°N, 99.30°W	533	Harney	Mixed grass prairie
		Restored prairie	38.84°N, 99.32°W			
		Agricultural field	38.84°N, 99.31°W			Wheat
Konza Long Term Ecological Research Station	Central	Native prairie	39.11°N, 96.61°W	865	Dwight-Irwin, Chase, Kennebec	Tallgrass prairie
		Restored prairie	39.10°N, 96.60°W			
		Agricultural field	39.10°N, 96.60°W			Maize
Welda Prairie	East	Native prairie	38.18°N, 95.27°W	1045	Ople-Kenoma	Tallgrass prairie
		Restored prairie	38.18°N, 95.27°W			
KSU East Central Experimental Field		Agricultural field	38.54°N, 95.25°W			Maize

2.2 Soil sampling and processing

In each plot, we sampled soils at multiple depths using a Giddings probe (Giddings Machine Company, Windsor, CO, USA). Individual plots had adjacent subplots for spring (June 2018) and fall (September 2018) sampling (Figure 1C). At both time points, cores were taken to a maximum depth of 150 cm, and then divided into five depth increments: 0-5 cm; 5-15 cm; 15-30 cm; 30-75 cm; and 75+ cm (Figure 1D). Maximum depth sampled was limited by equipment and rock layers at some sites. For example, deep soils in West sites allowed sampling to 150 cm, while Central and East sites were limited to 120 cm. In all downstream analyses, we consider these 75-120 cm and 75-150 cm soils to be part of a single depth increment, 75+ cm. Additionally, at the East native prairie site, a rock layer in the fall subplot prohibited sampling past 75 cm. At each sampling time, three soil cores (4 cm diameter) from each subplot were collected, then split by depth increment and pooled. For both spring and fall, this produced four pooled replicate samples for each depth, from each land use history, in each precipitation region. All soil samples were transported on ice to the nearest university, stored overnight at 4°C, then thoroughly homogenized and subsampled. We subsampled 25 g of soil for community sequencing, and stored these at -80°C until further processing.

2.3 Generation and processing of 16S and ITS amplicon sequencing libraries

Immediately prior to DNA extraction, we homogenized our 25 g molecular soil sample and subsampled 5 g of soil to ensure our DNA extraction was representative of the broader soil community (Kang and Mills, 2006; Song et al., 2015). Given the many different sample types and soils we collected, we tested multiple different protocols and kits to optimize DNA extraction for all samples. In this, we trialed ~14 different protocols on 0-5 cm and 75+ cm samples that had random combinations of annual precipitation and land use treatments. We selected the extraction methodology that allowed us to get as high a DNA concentration as possible, out of as many sample types as possible. Ultimately, we extracted total genomic DNA from 0.25 g of soil and from 1 blank (molecular-grade water) control per season using the DNeasy PowerSoil Pro Kit (Qiagen, Germantown, MD, USA), following the manufacturer's protocol. Extract quality and DNA concentration were assessed using the Qubit 2.0 Flourometer (Thermo Fisher Scientific, Waltham, MA, USA) High-Sensitivity dsDNA assay.

Despite our DNA extraction optimization, soil clay content was still too high in many samples to extract a workable quantity of DNA. This was especially the case in soils at the 30-75 cm depth and in soils deeper than 75 cm. Of the 356 total samples extracted, 17 (6 spring and 11 fall) had DNA concentrations less than 0.5 ng/mL. However, because prior efforts have indicated that some of these failed extractions could still produce useful sequencing libraries, we prepared libraries for all DNA extracts following the protocols detailed below, regardless of whether the extraction "failed." To sequence as many samples as possible without diluting our final library pool, we excluded samples that had a lower final DNA concentration than the blank control extraction at the amplicon purification step immediately prior to pooling. Further information on samples excluded from the final 16S and ITS pools is located in Table 2.

2.3.1 16S amplicon libraries

To generate bacterial community data, we amplified the V4 region of the 16S small subunit ribosomal gene using the Earth Microbiome Project (Thompson et al., 2017) primers combined with Illumina adaptor sequences. Our forward primer included the Illumina® (Illumina, Inc., San Diego, CA, USA) i5 overhang adapter sequence (5'-TCGTCGGCAGCGTCAGATGTGTATAAGAGACAG-3') attached to primer 515F-Y (5'-GTGYCAGCMGCCGCGGTAA-3'; Parada et al., 2016), and our reverse primer included the Illumina i7 overhang adapter sequence (5'-GTCTCGTGGGCTCGGAGATGTGTATAAGAGACAG-3') attached to primer 806R (5'-GGACTACNVGGGTWTCTAAT-3'; Apprill et al., 2015). Each 16S PCR reaction was prepared using 1X Q5® (New England Biolabs, Ipswich, MA, USA) reaction buffer, 1X Q5 GC enhancer, 0.02 U/µl High Fidelity (HF) Q5 polymerase, 2 mM dNTPs, 2 µM each forward and reverse primer, 1 µl DNA, and molecular-grade water to 25 µl. PCR amplifications consisted of a 30 s denaturation at 98°C; 25 cycles of 10 s at 98°C, 30 s at 57°C, and 30 s at 72°C; and a final elongation for 2 min at 72°C. 16S amplicons were then purified using the NucleoMag® PCR prep kit (Macherey-Nagel Gmbh & Co., Düren, Germany). Illumina Nextera™ indices were ligated to the purified amplicons in a second PCR reaction consisting of 1X Q5 reaction buffer, 1X Q5 GC enhancer, 0.02 U/µl Q5 HF polymerase, 0.3 mM dNTPs, 3 µl of each Nextera XT v2 index, 1 µl PCR product, and molecular-grade water to 50 µl. These amplifications consisted of a 30 s denaturation at 98°C; 8 cycles of 10 s at 98°C, 30 s at 55°C, and 30 s at 72°C; and a 5 min final elongation at 72°C. Amplicons were purified a second time using the NucleoMag PCR prep kit, and then pooled in equimolar concentrations in two groups that corresponded to samples taken in spring and fall seasons. We chose to pool and sequence samples when they were first available because we did not have enough Nextera index combinations to sequence all samples in a single pool. At the library pooling step, four and three samples were excluded from the spring and fall pools, respectively, because their final DNA concentrations were lower than the blank negative control (Table 2). Both pooled libraries were sequenced at the University of Kansas Genomic Sequencing Core (Lawrence, KS, USA) using Illumina 2x300 bp MiSeq v2 chemistry, resulting in 71,148 ± 20,223 and 86,905 ± 55,127 (mean ± sd) high-quality reads per sample in the spring and fall pools.

All 16S sequences were processed in QIIME2.10 (Bolyen et al., 2019). Demultiplexed sequences from fall and spring sequencing runs were denoised using the QIIME2 implementation of DADA2 (Callahan et al., 2016), and grouped into ASVs (amplicon sequence variants). We then combined outputs from both runs, and created a phylogenetic tree using the QIIME2 implementation of MAFFT fasttree (Price et al., 2010). Taxonomy was assigned to all ASVs by alignment to the SILVA database (Quast et al., 2013) using DADA2 in R version 3.6.2 (R Core Team, 2019). We conservatively removed all samples containing less than 1000 reads from the data set, as well as all non-reproducible ASVs (i.e., those that were observed less than 20 times and in under 5 samples). After sequence processing and quality filtering, our 16S data set comprised a total of 7836 ASVs in 165 spring and 169 fall samples (see Table 2).

2.3.2 ITS2 amplicon libraries

To generate fungal community data, we amplified the ITS2 region between the 5.8S and the 28S ribosomal genes. Our forward primer consisted of the Illumina i5 overhang adapter sequence attached to primer ITS7 (5'- GTGARTCATCGAATCTTTG-3', Ihrmark et al., 2012), and our reverse primer consisted of the Illumina i7 overhang adapter sequence attached to primer ITS4 (5'- TCCTCCGCTTATTGATATGC -3', White et al., 1990). Each ITS2 PCR reaction was prepared using 1X Q5 reaction buffer, 1X Q5 GC enhancer, 0.02 U/µl Q5 HF polymerase, 2 mM dNTPs, 2 µM each forward and reverse primer, 1 µl DNA, and molecular-grade water to 40 µl. From this point on, our ITS protocol is identical to our 16S protocol: We amplified ITS amplicons using the same thermocycling conditions, purified ITS amplicons using the NucleoMag PCR prep kit, and ligated Nextera indices using the reaction mix and thermocycling conditions described above. These PCR products were purified using the NucleoMag PCR prep kit once more, and pooled in equimolar concentrations in two groups that correspond to samples taken in the spring and fall. The spring pool excluded 6 and the fall pool excluded 7 samples with a final DNA concentration lower than the negative control (Table 2). Both pools were sequenced at the Kansas State University Genomic Sequencing Core (Manhattan, KS, USA) with Illumina 2x300 bp MiSeq v2 sequencing, resulting in 77,779 ± 19,124 and 86,365 ± 30,201 (mean ± sd) high-quality reads per sample in the spring and fall pools.

Like 16S sequences, all ITS2 reads were processed using QIIME2. Sequences from spring and fall sequencing runs were demultiplexed, denoised using the QIIME2 implementation of DADA2, and then combined. We grouped sequences into open reference OTUs (operational taxonomic units) at 97% sequence similarity using the UNITE database (Nilsson et al., 2019), and assigned taxonomy to all OTUs by alignment to UNITE using DADA2 in R. As with the 16S amplicon libraries, all non-reproducible OTUs and all samples containing less than 1000 reads were omitted from the data set. After sequence processing and quality filtering, our final ITS2 data set included 1925 OTUs across 168 spring and 166 fall samples (see Table 2).

Table 2. Number of samples from each treatment excluded at various steps in the library generation and sequence processing pipeline, as well as total number of samples with high-quality data included in statistical analyses. Treatments that have less than 4 replicates are highlighted in darker colors in the rightmost columns.

Region	Land use	Soil depth (cm)	Number of replicates sampled		Number of replicates excluded at library pooling				Number of replicates excluded at quality filtering				Total number of replicates included in final data set			
			Spring	Fall	Spring		Fall		Spring		Fall		Spring		Fall	
					16S	ITS	16S	ITS	16S	ITS	16S	ITS	16S	ITS	16S	ITS
West	Ag	0-5	4	4									4	4	4	4
West	Ag	5-15	4	4									4	4	4	4
West	Ag	15-30	4	4									4	4	4	4
West	Ag	30-75	4	4				1					4	4	4	3
West	Ag	75+	4	4	1	2	1	3	1				2	2	2	1
West	Restored	0-5	4	4									4	4	4	4
West	Restored	5-15	4	4									4	4	4	4
West	Restored	15-30	4	4									4	4	4	4
West	Restored	30-75	4	4									4	4	4	4
West	Restored	75+	4	4	1			1					3	4	4	3
West	Native	0-5	4	4									4	4	4	4
West	Native	5-15	4	4									4	4	4	4
West	Native	15-30	4	4									4	4	4	4
West	Native	30-75	4	4									4	4	4	4
West	Native	75+	4	4		1					1		4	3	3	4
Central	Ag	0-5	4	4					1	1			3	3	4	4
Central	Ag	5-15	4	4									4	4	4	4
Central	Ag	15-30	4	4									4	4	4	4
Central	Ag	30-75	4	4					1				3	4	4	4
Central	Ag	75+	4	4		1	2		1				3	3	2	4
Central	Restored	0-5	4	4									4	4	4	4
Central	Restored	5-15	4	4						1			4	3	4	4
Central	Restored	15-30	4	4						1			4	3	4	4
Central	Restored	30-75	4	4									4	4	4	4
Central	Restored	75+	4	4								2	4	4	4	2
Central	Native	0-5	4	4									4	4	4	4
Central	Native	5-15	3	4									3	3	4	4
Central	Native	15-30	4	4									4	4	4	4
Central	Native	30-75	4	4									4	4	4	4
Central	Native	75+	4	4		1							4	3	4	4
East	Ag	0-5	4	4									4	4	4	4
East	Ag	5-15	4	4									4	4	4	4
East	Ag	15-30	4	4								1	4	4	4	3
East	Ag	30-75	4	4						1			4	3	4	4
East	Ag	75+	4	4	1			1					3	4	4	3
East	Restored	0-5	4	4									4	4	4	4
East	Restored	5-15	4	4									4	4	4	4
East	Restored	15-30	4	4									4	4	4	4
East	Restored	30-75	4	4					1				4	4	4	4
East	Restored	75+	4	4	1				1		1		3	4	3	4
East	Native	0-5	4	4									4	4	4	4
East	Native	5-15	4	4									4	4	4	4
East	Native	15-30	4	4							1		4	4	3	4
East	Native	30-75	4	4				1					4	4	4	3
East	Native	75+	3	0		1			2				1	2	0	0

2.4 Statistical analyses

Unless noted, all analyses were performed using the package phyloseq (McMurdie and Holmes, 2013) through R (R Core Team, 2019), and were identical for bacteria and fungi. When applicable and as indicated below, we used Holm-Bonferroni and Tukey corrections to adjust *P*-values for multiple comparisons. In all cases, we assessed statistical significance at α=0.05.

We estimated alpha diversity by calculating Faith's PD for all bacterial samples using the R package btools (Battaglia, 2020), and the inverse of the Simpson Diversity Index (i.e., Inverse Simpson) for all fungal samples using phyloseq. We chose to use different measures of diversity for bacteria and fungi to account for differences between ASVs and OTUs; as ASVs represent sequence variants that differ by as much as one nucleotide, phylogenetic diversity measures like Faith's PD are needed to account for any sequences that may represent different strains of the same species (see Caruso et al., 2019). For statistical analyses of diversity, we used raw (unnormalized) ASV and OTU counts. Because analyses of community structure assume homoscedasticity and can be influenced by unequal variances (e.g., ordination), we normalized our ASV and OTU counts using log2 transformations for these analyses.

2.4.1 Defining within-season patterns of diversity and community structure

In defining patterns of diversity and community structure in individual seasons, we accounted for sequencing run biases by conducting separate analyses on our bacterial and fungal data sets by season, such that we had a total of four data sets: spring bacteria, fall bacteria, spring fungi, and fall fungi. We performed unconstrained PCoA on Bray-Curtis dissimilarities generated from log2-normalized ASV or OTU counts. Axes explaining the first cumulative ~50% of variation within each PCoA were extracted and used as response variables in generalized linear mixed models (GLMMs), along with the alpha diversity metrics described above. Outputs from models run on the first three axes of variation in each PCoA were used to assess statistical significance of variation in community structure; if a given factor had a statistically significant effect on any of the first three axes, we considered that factor to have significant impacts on community variation. Outputs from models run on all extracted axes were used to calculate the amount of community variation explained by the model's fixed predictors (within the first 50% of observed variation in the PCoA). We used this methodology to better account for variation associated with pseudoreplication of land use histories and spatial autocorrelation of our soil cores. Because traditional statistical methods of analyzing shifts in microbial community structure (e.g., PERMANOVA) are not able to properly account for variation associated with random effects, running analyses on individual PCoA axes allowed us to utilize univariate linear modeling methods that better control for random variation when assessing shifts in soil communities.

We fit all GLMMs using the R package lme4 (Bates et al., 2015). Each model included the fixed predictors 'soil depth,' 'land use,' 'region' (i.e., location along precipitation gradient), 'depth x land use,' and 'depth x region,' as well as the random predictors 'region x land use' and 'region x land use x plot.' These random predictors were included to account for pseudoreplication of land use types and for spatial autocorrelation of soil cores, respectively. To account for variation in sequencing depth, we included usable read count (i.e., read count at the conclusion of sequence processing and quality filtering) as a covariate in models applied to alpha diversity metrics only (see Glassman and Martiny, 2018). We assessed statistical significance of our fixed predictors using Type III ANOVAs with Satterthwaite's approximation of denominator degrees of freedom (lmerTest; Kuznetsova et al., 2017) and Holm-Bonferroni *P* value corrections, then investigated any significant differences with post-hoc pairwise comparisons and Tukey *P* value adjustments using emmeans (Lenth et al., 2020).

To determine the percent variation in community structure explained by each fixed predictor in our models (within the first ~50% of observed variation in each PCoA), we first multiplied the variation explained by the n^{th} axis, the variation explained by the n^{th} axis's GLMM (calculated using the package MuMIn; Bartoń, 2020), and the variation explained by each fixed predictor within that model. We then summed this value (i.e., the variation explained by a given predictor in the n^{th} axis) across all extracted axes. For example, to calculate the total amount of variation explained by the fixed predictor 'depth' in nine PCoA axes, we multiplied the variation explained by each axis with the variation explained by the GLMM run on each axis. We multiplied this value by the variation explained by depth in each ANOVA to get the total amount of community variation depth explained in each axis. We then summed these values across all nine axes to calculate the total amount of community variation explained by depth.

2.4.2 Comparing magnitudes of seasonal community change

We used the same data sets described above to evaluate differential magnitudes of seasonal change. While we expect sequencing run bias between spring and fall samples because they were sequenced in different groups, we do not expect that this bias differs among sample types. For instance, it is unlikely that biases between spring and fall agricultural samples are different from biases between spring and fall native samples. As such, although analyses directly comparing spring and fall communities could be distorted by sequencing run, it is possible to compare magnitudes of seasonal diversity and community structure change among sample treatments. We relied on this assumption to determine the precipitation regions, and land use histories, and soil depths where magnitudes of seasonal diversity and community structure shifts were greatest.

To assess magnitudes of seasonal diversity change, we subtracted fall diversity measures and usable read counts from spring. In doing so, we omitted 20 bacterial and 22 fungal sample pairs, mostly from the 30-75 cm and 75+ cm depth increments, that lacked high-quality data in either spring or fall (see Table 2). Because removing so many sample pairs resulted in a loss of statistical power and an inability to effectively test statistical significance associated with our deeper soil depths, we ran the GLMM described above on differences between spring and fall diversity metrics from the 0-5 cm, 5-15 cm, and 15-30 cm depth increments only. We assessed statistical significance of fixed predictors using Type III ANOVA, and investigated significant differences with post-hoc pairwise comparisons and Tukey *P* value adjustments.

To assess magnitudes of seasonal shifts in community structure, we calculated the distance between spring-fall pairs of Bray-Curtis dissimilarities. Because we once again had to remove 20 bacterial and 22 fungal sample pairs, mostly from the 30-75 cm and 75+ cm depth increments, we included only 0-5 cm, 5-15 cm, and 15-30 cm depths in these analyses as well. We ran the GLMM on distances between spring and fall samples in the top three depth increments only. We assessed statistical significance of fixed predictors using Type III ANOVA, and investigated significant differences with post-hoc pairwise comparisons and Tukey *P* value adjustments.

3 Results

3.1 Factors driving within-season diversity differ between bacteria and fungi

To determine the degree to which microbial diversity is influenced by precipitation, land use, and soil depth in individual seasons, we ran GLMMs on bacterial Faith's PD and fungal Inverse Simpson diversity measures. In all cases, usable read count had a significant effect on diversity (Table 3), explaining 39.7% and 53.3% of the total variation in spring and fall bacterial diversity, and 3.2% and 3.7% of the total variation in spring and fall fungal diversity, respectively.

After accounting for this sampling effect, bacterial phylogenetic diversity was explained by depth in both seasons (spring $F_{4,112}$=12.38, P=2.2e-8; fall $F_{4,113}$=8.76, P=3.4e-6). Depth explained 12.2% of the total variation in diversity in the spring and 14.2% of the total variation in the fall, but phylogenetic diversity did not show relationships to precipitation, land use, or any combination of these fixed factors (Table 3). Bacterial phylogenetic diversity followed identical trends across both seasons. Diversity was greatest at 5-15 cm depth increment and lowest at depths deeper than 75 cm. (Figure 2A; Table S1).

Fungal diversity was similarly explained by soil depth (spring $F_{4,142}$=10.73, P=1.2e-7; fall $F_{4,141}$=4.44, P=0.002; Table 3), with depth explaining 16.0% of the total variation in fungal Inverse Simpson in the spring, and 8.0% in the fall. Diversity in both seasons was highest and most variable at the deepest soil depths (Figure 2B; Table S2). In contrast to bacterial phylogenetic diversity, historical precipitation also shaped fungal diversity, as evidenced by a significant effect of region (spring $F_{4,142}$=10.73, P=1.2e-7; fall $F_{4,141}$=4.44, P=0.002) and the interaction depth x region (spring $F_{4,112}$=12.38, P=2.2e-8; fall $F_{4,113}$=8.76, P=3.4e-6; Table 3). Region and depth x region explained 5.9% and 7.0% of the total variation in diversity in the spring, and 8.3% and 11.0% in the fall, respectively. In both seasons, diversity across the precipitation gradient was most similar between 0 and 30 cm, and began to diverge at deeper depths, with West, 75+ cm soils having the highest diversity overall, and Central, 75+ cm soils having the lowest (Figure 2C, 2D; Table S2).

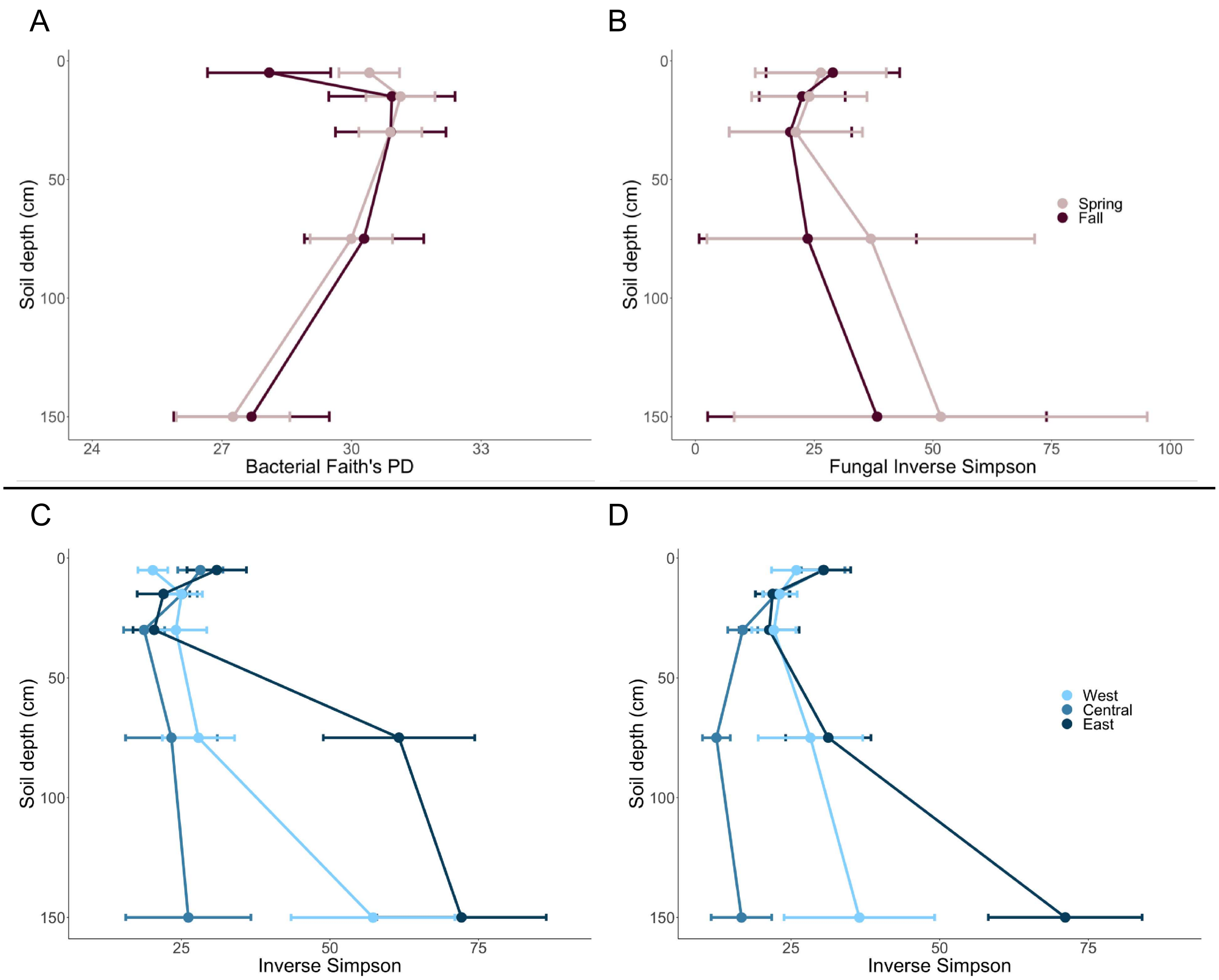

Figure 2. Microbial diversity throughout the soil profile. In each panel, the x-axis represents diversity and the y-axis represents soil depth, with deeper depths being plotted towards the bottom of the axis. Points along the y-axis represent the maximum depth sampled in each depth increment. For instance, because soils in the 75+ cm increment were sampled to a maximum depth of 150 cm, points at 150 cm represent the 75+ cm increment. Points and error bars represent means and standard error, respectively. The top two panels depict shifts in **(A)** bacterial Faith's PD and **(B)** fungal Inverse Simpson across seasons, with colors in both panels representing spring and fall. The bottom two panels separate changes in fungal Inverse Simpson in **(C)** the spring and **(D)** the fall across precipitation regions. Colors in both (C) and (D) are representative of West, Central, and East precipitation regions.

Table 3. Model R^2 and *P* values from ANOVAs applied to LMMs run on diversity measurements.

	Bacteria (Faith's PD)		**Fungi (Inverse Simpson)**	
	Spring	**Fall**	**Spring**	**Fall**
Model R^2	0.733	0.859	0.381	0.379
Usable read count	$F_{1,129}$=161.95 **P<2.2e-16 *****	$F_{1,42}$=151.68 **P=1.5e-15 *****	$F_{1,142}$=8.48 **P=0.0042 ****	$F_{1,141}$=8.29 **P=0.0046 ****
Soil depth	$F_{4,112}$=12.38 **P=2.2e-8 *****	$F_{4,112}$=8.76 **P=3.9e-6 *****	$F_{4,142}$=10.73 **P=1.25e-7 *****	$F_{4,141}$=4.44 **P=0.0021 ****
Region	$F_{2,4}$=1.32 P=0.36	$F_{2,4}$=0.28 P=0.79	$F_{2,142}$=7.93 **P=0.0005 *****	$F_{2,141}$=9.23 **P=0.0002 *****
Depth x region	$F_{8,112}$=1.77 P=0.09	$F_{8,112}$=0.89 P=0.53	$F_{8,142}$=2.34 **P=0.021 ***	$F_{8,141}$=3.05 **P=0.0034 ****
Land use history	$F_{2,4}$=3.32 P=0.14	$F_{2,4}$=3.79 P=0.12	$F_{2,142}$=2.68 P=0.072	$F_{2,141}$=0.066 P=0.94
Depth x land use	$F_{8,112}$=1.50 P=0.16	$F_{8,112}$=1.10 P=0.37	$F_{8,142}$=1.36 P=0.22	$F_{8,141}$=1.92 P=0.061

3.2 Bacterial and fungal communities are structured by similar factors across seasons

To determine how microbial communities are structured across the precipitation gradient, land use histories, and soil depths, we applied GLMMs to axes representing the first ~50% of community variation in PCoAs representing spring and fall bacteria, and spring and fall fungi. We used the GLMMs run on the first three axes of each PCoA to predict statistical significance of our fixed predictors. We then used the GLMMs run on all extracted axes to assess the total amount of community variation explained by our model's fixed predictors.

Of our five fixed predictors, land use was the only factor that did not significantly contribute to variation in spring bacterial communities. The first three PCoA axes explained 14.2%, 9.9%, and 8.0% of the variation in spring bacterial communities, and all three were predicted by soil depth and the interaction depth x region. The first axis was also predicted by region, and the second by the interaction depth x land use (Figure 3A; Table 4). Within the first nine PCoA axes (explaining the first 52.1% of bacterial community variation), soil depth predicted 21.5% of total bacterial community variation, the interaction depth x region interaction explained 10.7%, the interaction depth x land use explained 2.6%, and region explained 1.5% (Figure 3A; Table S3).

Bacterial communities in the fall were structured similarly to those in the spring. Of our five fixed predictors, both region and land use did not contribute to variation in fall bacterial communities. The first three PCoA axes explained 11.4%, 9.6%, and 7.5% of fall bacterial community variation, and were all predicted by soil depth and by the interaction depth x region. The second and third axes were also predicted by the depth x land use interaction (Figure 3B; Table 4). Within the first ten PCoA axes (explaining the first 51.1% of community variation), soil depth explained 18.1% of the total bacterial community variation in the fall, the interaction depth x region explained 8.7%, and the interaction depth x land use explained 3.4% (Figure 3B; Table S4).

Table 4. Model R^2 values and Holm-Bonferroni corrected *P* values from ANOVAs applied to LMMs run on the first 3 axes of variation in spring and fall bacterial PCoAs.

	Spring			Fall		
	PCo1	**PCo2**	**PCo3**	**PCo1**	**PCo2**	**PCo3**
Model R^2	0.933	0.919	0.824	0.876	0.904	0.848
Soil depth	$F_{4,112}$=12.38 **P=1.5e-45 *****	$F_{4,112}$=8.76 **P=1.3e-58 *****	$F_{4,112}$=12.38 **P=1.0e-25 *****	$F_{4,142}$=10.73 **P=1.1e-40 *****	$F_{4,141}$=4.44 **P=4.8e-40 *****	$F_{4,112}$=12.38 **P=1.1e-26 *****
Region	$F_{2,4}$=1.32 **P=0.049 ***	$F_{2,4}$=0.28 P=0.053	$F_{2,4}$=1.32 P=0.67	$F_{2,142}$=7.93 P=0.47	$F_{2,141}$=9.23 P=0.55	$F_{2,4}$=1.32 P=0.74
Depth x region	$F_{8,112}$=1.77 **P=1.0e-24 *****	$F_{8,112}$=0.89 **P=0.0034 ****	$F_{8,112}$=0.89 **P=4.6e-28 *****	$F_{8,142}$=2.34 **P=3.1e-13 *****	$F_{8,141}$=3.05 **P=0.0021 ****	$F_{8,112}$=0.89 **P=1.1e-17 *****
Land use history	$F_{2,4}$=3.32 P=1.0	$F_{2,4}$=3.79 P=1.0	$F_{2,4}$=1.32 P=1.0	$F_{2,142}$=2.68 P=1.0	$F_{2,141}$=0.066 P=1.0	$F_{2,4}$=1.32 P=1.0
Depth x land use	$F_{8,112}$=1.50 P=0.060	$F_{8,112}$=1.10 **P=0.0001 *****	$F_{8,112}$=0.89 P=0.059	$F_{8,142}$=1.36 P=0.31	$F_{8,141}$=1.92 **P=0.041 ***	$F_{8,112}$=0.89 **P=3.6e-12 *****

The fixed predictors that contributed to bacterial community variation were similar to those that contributed to fungal community variation. For instance, bacterial and fungal communities were explained by the same fixed predictors in the spring, expect that region did not explain variation in fungal communities. The first three spring fungal PCoA axes explained 14.0%, 12.5%, and 10.4% of the total community variation. All three of these axes were predicted by soil depth and by the depth x region interaction. The third axis was also predicted by the interaction depth x land use (Figure 3C; Table 5). Compared to bacterial communities, these fixed predictors explained less total variation in fungal communities. Within the first six spring fungi PCoA axes (explaining the first 50.4% of spring fungal community variation), soil depth explained 13.9% of the total fungal community variation, the interaction depth x region explained 7.5%, and the interaction depth x land use explained 5.3% (Figure 3C; Table S5).

Fall fungal communities were explained by fixed predictors similar to those in the spring. The first three fall fungal PCoA axes explained 15.0%, 11.3%, and 7.0% of the total community variation, and all three axes were predicted by soil depth and the depth x land use interaction. The second and third axes were also predicted by the interaction depth x region (Figure 3D; Table 5). Within the first 8 PCoA axes (explaining 51.1% of fall fungal community variation), soil depth explained 21.8% of total fall fungal community variation, the interaction depth x land use explained 4.8%, and the interaction depth x region explained 3.6% (Figure 3D; Table S6).

Table 5. Model R^2 values and Holm-Bonferroni corrected *P* values from ANOVAs applied to LMMs run on the first 3 axes of variation in spring and fall fungal PCoAs.

	Spring			**Fall**		
	PCo1	**PCo2**	**PCo3**	**PCo1**	**PCo2**	**PCo3**
Model R^2	0.739	0.860	0.773	0.894	0.921	0.913
Soil depth	$F_{4,112}$=12.38 ***P*=2.5e-6 *****	$F_{4,112}$=8.76 ***P*=9.7e-16 *****	$F_{4,112}$=8.76 ***P*=3.1e-38 *****	$F_{4,142}$=10.73 ***P*=1.0e-44 *****	$F_{4,141}$=4.44 ***P*=1.3e-31 ****	$F_{4,112}$=8.76 ***P*=1.3e-42 *****
Region	$F_{2,4}$=1.32 *P*=0.76	$F_{2,4}$=0.28 *P*=0.48	$F_{2,4}$=0.28 *P*=1.0	$F_{2,142}$=7.93 *P*=1.0	$F_{2,141}$=9.23 *P*=0.23	$F_{2,4}$=0.28 *P*=0.69
Depth x region	$F_{8,112}$=1.77 ***P*=4.3e-7 *****	$F_{8,112}$=0.89 ***P*=1.6e-7 *****	$F_{8,112}$=1.50 ***P*=0.0004 *****	$F_{8,142}$=2.34 *P*=0.17	$F_{8,141}$=3.05 ***P*=4.3e-8 *****	$F_{8,112}$=1.50 ***P*=3.7e-8 *****
Land use history	$F_{2,4}$=3.32 *P*=0.95	$F_{2,4}$=3.79 *P*=0.20	$F_{2,4}$=0.28 *P*=1.0	$F_{2,142}$=2.68 *P*=0.35	$F_{2,141}$=0.066 *P*=1.0	$F_{2,4}$=0.28 *P*=0.59
Depth x land use	$F_{8,112}$=1.50 *P*=0.061	$F_{8,112}$=1.10 ***P*=1.5e-8 *****	$F_{8,112}$=1.50 *P*=0.061	$F_{8,142}$=1.36 ***P*=4.3e-13 *****	$F_{8,141}$=1.92 ***P*=0.0004 *****	$F_{8,112}$=1.50 ***P*=1.6e-15 *****

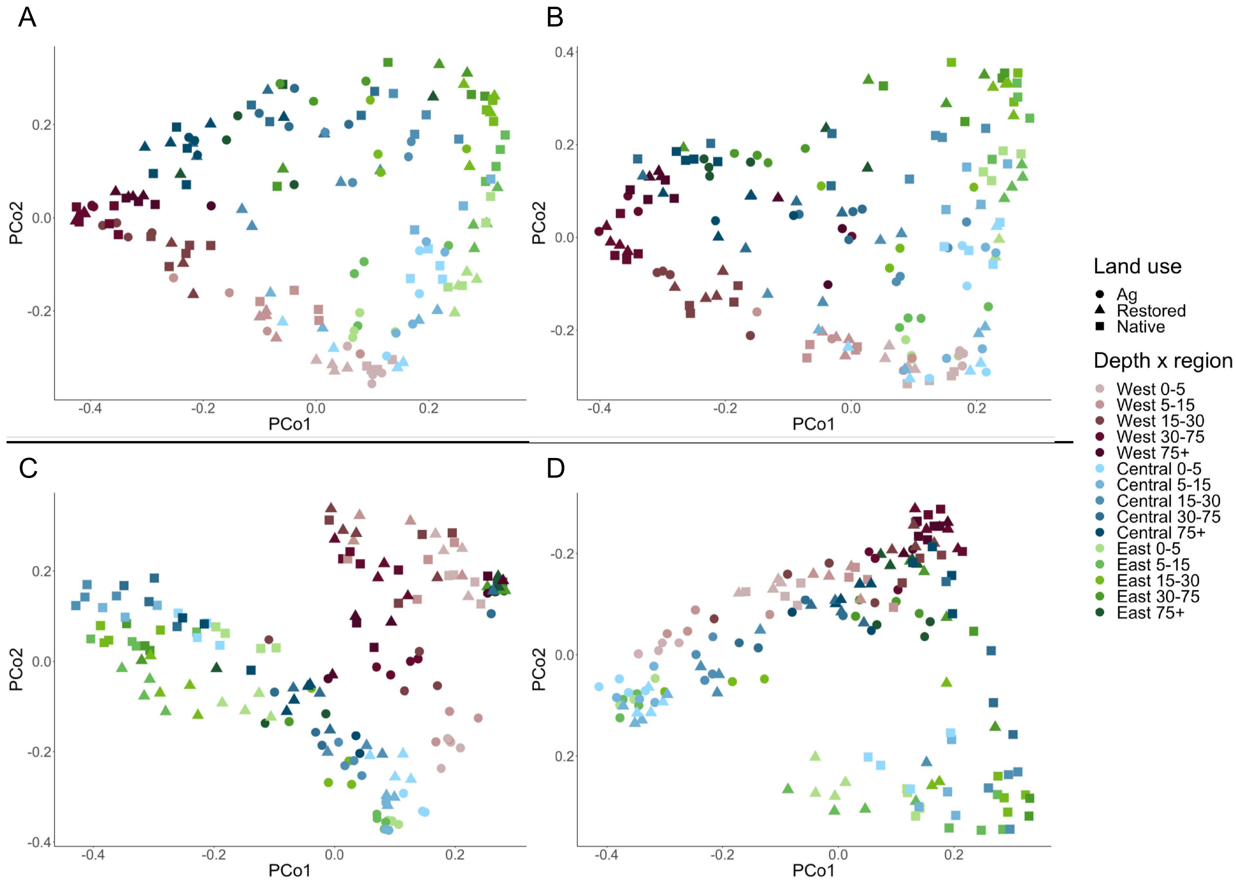

Figure 3. PCoA of **(A)** spring bacteria, **(B)** fall bacteria, **(C)** spring fungi, and **(D)** fall fungi. In all panels, PCo1 axes are plotted on the x-axis, and PCo2 axes are plotted on the y-axis. Light colors indicate surficial soil depths, while dark colors indicate deeper depths. Shapes are representative of land use history, and colors are representative of annual precipitation. Because PCoA axis direction is arbitrary, the y-axis in (D) is reversed to maintain consistency with panel (C).

3.3 Magnitudes of seasonal diversity change are negligible for bacteria and fungi

We assessed magnitudes of seasonal diversity change by running GLMMs on the differences between spring and fall measures of diversity (i.e., Faith's PD and Inverse Simpson) from the top three depth increments only. Difference in usable read count had a significant effect on magnitudes of seasonal changes in bacterial phylogenetic diversity, explaining 69.9% of the total variation in bacterial diversity shifts. However, read count did not influence measures of seasonal change in fungal diversity (Table 6).

After accounting for this sampling effect, seasonal changes in bacterial diversity were predicted by soil depth ($F_{2,61}$=4.01, P=0.023), but no other fixed predictors. Bacterial phylogenetic diversity increased more from spring to fall in the 0-5 cm than at 15-30 cm (t_{62}=-2.64, P=0.028; Table S7), with diversity change at 5-15 cm being intermediate. While significant, the effect of soil depth explained only 3.0% of the total variation in seasonal changes in phylogenetic diversity. Seasonal shifts in fungal Inverse Simpson were not explained by any fixed predictors (Table 6).

Table 6. Model R^2 and P values from ANOVAs applied to GLMMs run on magnitudes of seasonal diversity change.

	Seasonal change in Faith's PD	**Seasonal change in Inverse Simpson**
Model R^2	0.858	0.066
Usable read count	$F_{1,13}$=185.10 **P=6.2e-9 *****	$F_{1,88}$=0.0018 P=0.97
Soil depth	$F_{2,61}$=4.01 **P=0.023 ***	$F_{2,88}$=0.45 P=0.64
Region	$F_{2,4}$=1.17 P=0.40	$F_{2,88}$=0.040 P=0.96
Depth x region	$F_{4,61}$=2.29 P=0.069	$F_{4,88}$=0.20 P=0.94
Land use history	$F_{2,4}$=0.0087 P=0.99	$F_{2,88}$=0.72 P=0.49
Depth x land use	$F_{4,61}$=2.37 P=0.062	$F_{4,88}$=0.95 P=0.44

3.4 Seasonal shifts in bacterial and fungal community structure differ with depth and precipitation region

We assessed magnitudes of seasonal change in bacterial and fungal community structure by calculating the distance between spring and fall Bray-Curtis dissimilarities, such that greater distances represent larger magnitudes of seasonal change in community structure. Similar to analyses of seasonal diversity change, we ran GLMMs on distances from only the 0-5 cm, 5-15 cm, and 15-30 cm depth increments.

Magnitudes of seasonal shifts in bacterial community structure were predicted by soil depth ($F_{2,61}$=38.58, P=1.4e-11; Table 7), with depth explaining 33.0% of the total variation in community structure shifts. As with diversity, distances between spring and fall community structure were greatest at the 0-5 cm depth increment (Figure 5A; Table S8). These distances were also shaped by the interaction depth x region ($F_{4,62}$=4.12, P=0.0051; Table 7), which explained 7.1% of the total variation in seasonal shifts in bacterial community structure. Magnitudes of seasonal change among precipitation regions were most distinct at the top of the soil profile, and became more similar with increasing soil depth (Figure 5B; Table S8).

Seasonal changes in fungal community structure were predicted by region ($F_{2,4}$=9.05, P=0.032; Table 7), with historic annual precipitation explaining 12.6% of the total variation in fungal community structure shifts. Distances between spring and fall communities were greater in East and West regions than in the Central region (Figure 5C; Table S9). Like bacterial communities, seasonal change in fungal community structure was also shaped by the interaction depth x region ($F_{4,59}$=6.55, P=0.0002; Table 7), which explained 18.2% of the total variation in seasonal fungal community shifts. Seasonal shifts in fungal communities were most distinct between Central and West regions at the top of the soil profile, and became more variable with increasing soil depth (Figure 5D; Table S8).

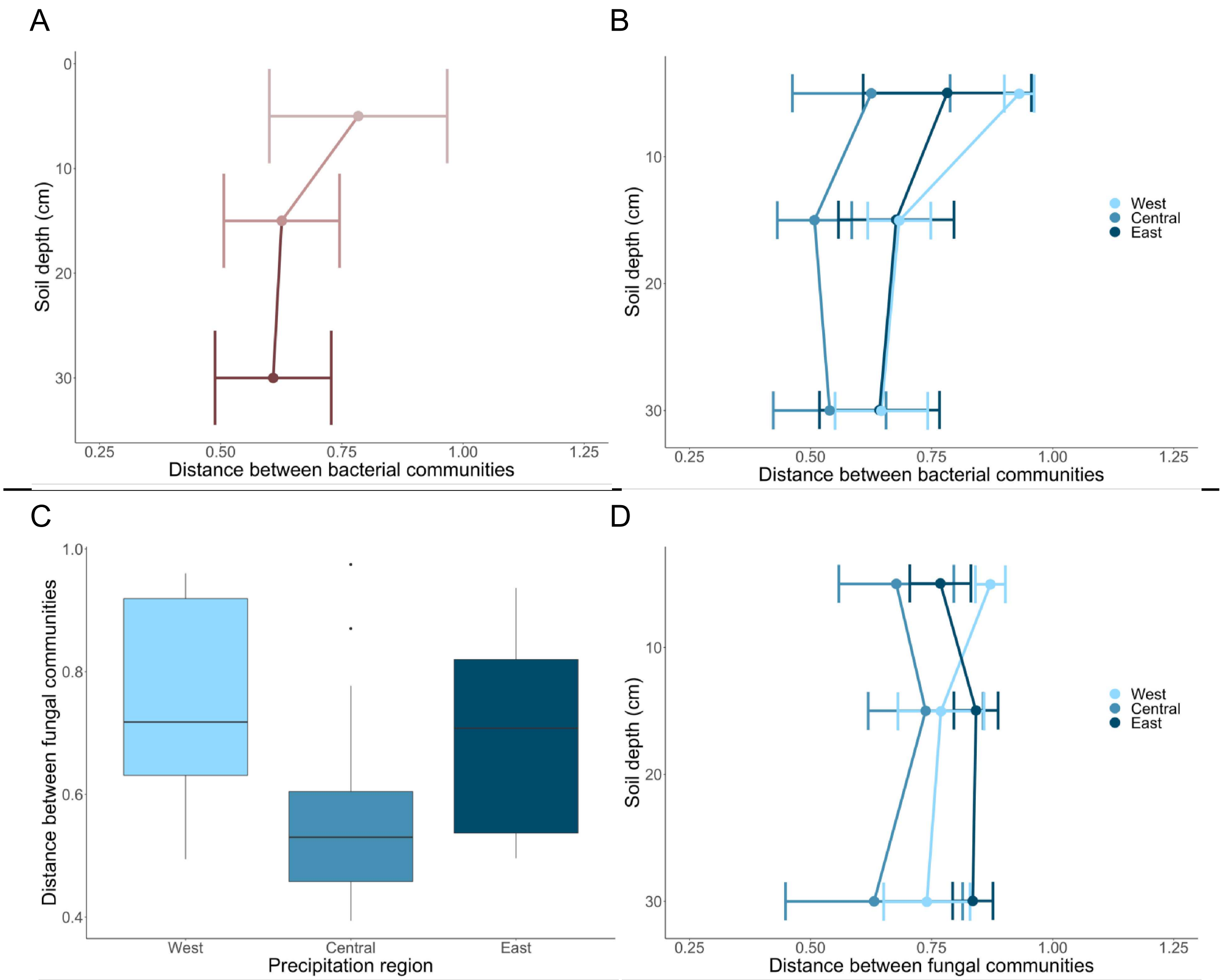

Figure 4. Magnitudes of seasonal change in bacterial and fungal community structure. The top two panels depict magnitudes of seasonal shifts in bacterial community structure with **(A)** soil depth and **(B)** the interaction soil depth x precipitation region. The bottom two panels depict shifts in fungal community structure with **(C)** precipitation region and **(D)** the interaction soil depth x precipitation region. In (A), (B), and (D), the x-axis represents distance between spring and fall Bray-Curtis dissimilarity indices, and the y-axis represents soil depth, with points along this axis representing the maximum depth sampled in each depth increment. In (C), the x-axis represents precipitation region, and the y-axis represents distance between spring and fall communities. Colors in both (B), (C), and (D) are representative of West, Central, and East precipitation regions.

Table 7. Model R^2 and *P* values from ANOVAs applied to GLMMs run on magnitudes of seasonal shifts in community structure.

	Distance between spring and fall bacterial communities	**Distance between spring and fall fungal communities**
Model R^2	0.752	0.582
Soil depth	$F_{2,61}$=38.56 ***P*=1.4e-11 *****	$F_{2,60}$=3.08 *P*=0.053
Region	$F_{2,4}$=2.93 *P*=0.16	$F_{2,4}$=9.05 ***P*=0.032 ***
Depth x region	$F_{4,62}$=4.12 ***P*=0.0051 ****	$F_{4,59}$=6.55 ***P*=0.0002 *****
Land use history	$F_{2,4}$=0.049 *P*=0.95	$F_{2,4}$=0.67 *P*=0.57
Depth x land use	$F_{4,61}$=1.88 *P*=0.13	$F_{4,59}$=1.24 *P*=0.30

4 Discussion

In this study, we assessed how within-season variation in microbial community diversity and structure, as well as how seasonal shifts in these measures, vary along gradients of climate (represented by precipitation), land use history, and soil depth. We found that within-season variation in bacterial and fungal communities responded similarly to gradients of annual precipitation, land use, and soil depth, with depth explaining the majority of variation in diversity and community structure overall. Additionally, while seasonal shifts in diversity were only observed in bacterial communities at the 0-5 cm depth, seasonal community structure changes in bacterial and fungal communities at this depth largely depended on annual precipitation. Overall, this indicates that while soil depth plays a large role in describing within-season community variation, precipitation most strongly influences how communities change over seasons, especially in the upper layers of the soil.

4.1 Factors influencing within-season variation in diversity and community structure

As mentioned, soil depth explained the majority of diversity and community structure variation in bacterial and fungal communities. In particular, fungal diversity was most variable at deeper soil depths. Our findings align with multiple studies on microbial community variation throughout the soil profile (Eilers et al., 2012; Fierer et al., 2003; Hao et al., 2020; Jumpponen et al., 2010; Will et al., 2010). Soil structure, pH, nutrient availability, and root abundance shift rapidly with depth (Eilers et al., 2012; Jobbágy and Jackson, 2001; White and Kirkegaard, 2010), and exert strong influences on bacterial and fungal communities (Broeckling et al., 2008; Fierer and Jackson, 2006; Glassman et al., 2017). As such, microbial community variation may mirror the steep environmental gradients present in the soil profile. Bulk density and soil carbon content may be especially important drivers of depth-related community variation, as both of these soil properties have been shown to explain significant portions of depth-related community variation in multiple environments (Eilers et al., 2012; Fierer et al., 2003; Hao et al., 2020). We note that deep soils can be challenging to sample, and that extracting high-quality DNA from these samples can be problematic. Combined, these challenges limit our ability to asses microbial community variation with depth. While we accounted for these missing data from deep soils statistically (replication and read counts), more high-quality data from the deeper soils of the Central Plains is needed to better confirm these general patterns.

Precipitation also explained variation in soil communities throughout the soil profile. However, the degree to which precipitation influenced microbial community diversity and structure differed between bacteria and fungi. Precipitation played a stronger role in shaping fungal than bacterial diversity. With regards to community structure, precipitation had significant effects on both bacteria and fungi throughout the soil profile, though our findings demonstrate that precipitation effects were more pronounced for bacterial than fungal communities. Precipitation explained about twice as much variation in bacterial than in fungal communities, a finding that was consistent in both spring and fall. In both communities, approximately one-third more variation was explained by precipitation in the spring than the fall. This is likely because our spring sampling occurred when precipitation differences among West and East/Central regions were most distinct (see Figure S1). Our findings of precipitation-driven variation in both community diversity and structure reflect our current understanding of how bacterial and fungal life histories shape their response to precipitation. Bacteria rely more on soil water availability as a habitat and in dispersal (Barnard et al., 2013), which makes them more sensitive to precipitation differences. In contrast, apical growth in fungal hyphae allows them to spread across dry gaps in soil particles and better resist changes in soil moisture (Bapiri et al., 2010). As such, while both kingdoms respond to changes in precipitation (Hawkes et al., 2011; Waring and Hawkes, 2018), bacterial community structure, but not necessarily diversity (Angel et al., 2010; Bachar et al., 2010; Wang et al., 2015), may respond more than fungal communities (de Vries et al., 2018).

Land use history played a minor, albeit significant role in shaping both bacterial and fungal community structure throughout the soil profile. It did not, however, shape the diversity of either kingdom. This indicates that land use drives some community turnover, but not necessarily diversity changes, in bacterial and fungal communities. Microbial community shifts as a result of land use history are well-supported across multiple ecosystem types (Osburn et al., 2019; Steenwerth et al., 2002; Xiang et al., 2014). While significant, land use played a small role in shaping communities compared to the effects of precipitation and depth. In both seasons, land use contributed to only ~3% of the differences in bacterial and ~5% in fungal community structure. Given the close relationships between microbial communities and the many soil properties associated with land use history (Xiang et al., 2014), we expected the amount of community variation explained by land use to be higher overall. As our experimental design required averaging community variation with land use over variation associated with annual precipitation, this might indicate that variables most closely associated with precipitation, like soil moisture and pH (Slessarev et al., 2016), contribute more to community variation than variables that differ with land use. This could be especially true in Kansas, where rich Mollisols provide an abundance of soil nutrients, regardless of land use history (Hatfield et al., 2017). The absence of this limiting factor could mean that the competitive interactions for resources that play a role in community change (Litchman et al., 2015) are somewhat lessened.

Though it is possible that the mechanisms detailed above contribute to our observed patterns of community variation, it is very likely that pseudoreplication of land use types played an equal or greater role in driving these patterns. Though we accounted for this variation statistically, it remains a significant barrier to accurately delimiting the relative influences of precipitation, land use history, and soil depth on microbial communities at the landscape scale. Though unavoidable in this study, sacrificial pseudoreplication can increase chances of detecting false negatives (Hurlbert, 1984). Given land use's well-established role in shaping soil bacterial and fungal communities, this phenomenon is likely present in our study. As such, our sampling design may be limiting our ability to realize land use's true impacts on communities, and historical land use likely has a greater impact on microbial communities than what we were able to detect.

4.2 Comparing magnitudes of seasonal community change

Contrary to our predictions, only soil depth and precipitation shaped magnitudes of bacterial and fungal community change across the growing season. While precipitation explained seasonal changes in bacterial and fungal community structure throughout the soil profile, these changes were most pronounced at the 0-5 cm depth. This comes despite strong seasonal changes in root growth and exudates throughout the profile (Canarini et al., 2019; Williams and Vries, 2020), and is likely due to soil's ability to insulate subsurface communities from environmental perturbations like seasonal changes in precipitation. This finding is supported by other work in grasslands showing that bacteria and fungi at the soil's surface shift more over seasons than communities at deeper depths (Griffiths et al., 2003). The idea that surficial communities are most exposed and sensitive to environmental perturbations extends across the literature. With a wide variety of disturbance types, including land modification (Hartmann et al., 2009) and prescribed fire (Semenova‐Nelsen et al., 2019), surficial bacterial and fungal communities are more impacted than those deeper within the soil profile.

While land use shaped bacterial and fungal community structure in individual seasons, it did not impact differences across seasons with either community. We hypothesized that cropping and fertilization would create greater seasonal change in communities in agricultural systems. Alternatively, we also hypothesized that competitive interactions with greater roots and fewer mineral nutrients would drive larger seasonal changes in native systems. Neither hypothesis was correct: communities in native, restored, and agricultural systems showed, on average, similar changes in diversity and community structure over the growing season. This finding might be derived from the timing of our sampling. Sampling in June and September did not allow us to detect community variation prior to planting and fertilization, or after harvest; June sampling occurred several months after fertilizer application and planting, and September sampling occurred before crops were harvested. Both of these anthropogenic influences shape seasonal community variation in agricultural systems, with comparatively little community change occurring independently of these disturbances (Hamel et al., 2006; Shi et al., 2013). In light of this, our findings make sense, and indicate that more frequent and expanded sampling across the year might detect the seasonal community variation with land use found in other studies.

These findings should be interpreted with caution, as the statistical methods we used to determine magnitudes of community change across seasons are fairly conservative. It is possible that differences in seasonal community shifts found at the 0-5 cm depth are greater in reality than revealed by our methods. Likewise, it is also possible that magnitudes of seasonal community shifts do diverge at other points in the soil profile, as well as with land use history. In combination with pseudoreplication of land use types, this limits our ability to make more comprehensive conclusions on soil bacterial and fungal community change across seasons. Though our methods were able to describe some seasonal changes in soil microbial communities, analyses including data generated with minimizing sequencing run bias in mind (i.e., spreading samples from different time points across different sequencing runs), as well as data from additional seasons like summer, are needed to more accurately and precisely determine the environmental conditions governing seasonal change in microbial communities.

4.3 Considerations for future research

Our work highlights the importance of soil depth when assessing soil microbial response to climate, environmental gradients, and disturbance, whether at a single time or across seasons. Because bacterial and fungal communities varied most distinctly with soil depth, homogenizing whole soil cores, especially those deeper than 5 cm, likely masks relevant community variation. For example, in studies assessing impacts of environmental disturbance on microbial communities (e.g., McKenna et al., 2020), homogenizing whole cores could lessen the ability to detect the effects of that disturbance. This could be particularly true if that disturbance is predicted to impact only communities in the top layers of the soil. While sampling deep into the soil profile is not always necessary (or possible), dividing soil cores into depth increments or soil horizons is already recognized by soil scientists as critical. Doing so to assess soil microbial communities could preserve community variation with depth that is relevant to correctly assessing the strength of environmental changes.

4.4 Role of broad categories to describe fundamental variables shaping microbial communities at the landscape scale

Overall, our findings indicate that within-season community variation is shaped primarily by soil depth, with precipitation and land use history playing a lesser role. We also found that seasonal community change is described primarily by average annual precipitation within the top 5 cm of soil. Given these findings, we might hypothesize that community variation, both within a single season and across a growing season, is shaped most strongly by variables that correlate with differences in depth and annual precipitation. As highlighted above, these variables might include bulk density, soil moisture, pH, and organic carbon content. Future work includes assessing how bacterial and fungal diversity and community structure differ with these variables, along with measures of multiple other plant and soil properties across these gradients.

Although our broad environmental categories were useful in describing general patterns of bacterial and fungal community variation, they are derived from an anthropogenic perspective. As such, they do not allow us to make specific predictions about how variation in microbial community diversity and structure relate to community function. Variation in both fungal and bacterial communities correlate more strongly with variation in specific soil properties than with broad land use and climate categories (Bachelot et al., 2016; Delgado□Baquerizo et al., 2016; Xiang et al., 2014), with relatively fine-scale variation in these properties explaining more than 50% of community variation at the continental scale (Averill et al., 2019; Fierer and Jackson, 2006). As such, using broad categories for assessments of community variation could inhibit detection of biologically relevant variation in communities, especially at large spatial scales. Microbial communities interact with their environment at a microscale, where their ability to interface with variations in nutrient availability, pH, soil moisture, and multiple other soil properties may more closely determine their ability to perform ecosystem functions than broad environmental categories. As such, assessments of bacterial and fungal community variation would benefit from utilizing gradients of soil properties to relate microbial communities in the context of the ecosystem services they provide. To understand where seasonal changes in diversity and community structure matter most, we should look to their associated impacts on potential changes in microbial function. Because microbial communities are intimately linked with ecosystem function (Philippot et al., 2013; Strickland et al., 2009), both small and large magnitudes of community change could have implications for microbial function at the ecosystem scale and subsequently, the ecosystem services upon which we rely.

5 References

Angel, R., Soares, M.I.M., Ungar, E.D., Gillor, O., 2010. Biogeography of soil archaea and bacteria along a steep precipitation gradient. ISME J. 4, 553–563.

Apprill, A., McNally, S., Parsons, R., Weber, L., 2015. Minor revision to V4 region SSU rRNA 806R gene primer greatly increases detection of SAR11 bacterioplankton. Aquat. Microb. Ecol. 75, 129–137.

Averill, C., Cates, L.L., Dietze, M.C., Bhatnagar, J.M., 2019. Spatial vs. temporal controls over soil fungal community similarity at continental and global scales. ISME J. 13, 2082–2093.

Averill, C., Waring, B.G., Hawkes, C.V., 2016. Historical precipitation predictably alters the shape and magnitude of microbial functional response to soil moisture. Glob. Change Biol. 22, 1957–1964.

Bachar, A., Al-Ashhab, A., Soares, M.I.M., Sklarz, M.Y., Angel, R., Ungar, E.D., Gillor, O., 2010. Soil Microbial Abundance and Diversity Along a Low Precipitation Gradient. Microb. Ecol. 60, 453–461.

Bachelot, B., Uriarte, M., Zimmerman, J.K., Thompson, J., Leff, J.W., Asiaii, A., Koshner, J., McGuire, K., 2016. Long-lasting effects of land use history on soil fungal communities in second-growth tropical rain forests. Ecol. Appl. 26, 1881–1895.

Bapiri, A., Bååth, E., Rousk, J., 2010. Drying-rewetting cycles affect fungal and bacterial growth differently in an arable soil. Microb. Ecol. 60, 419–428.

Bardgett, R.D., Lovell, R.D., Hobbs, P.J., Jarvis, S.C., 1999. Seasonal changes in soil microbial communities along a fertility gradient of temperate grasslands. Soil Biol. Biochem. 31, 1021–1030.

Barnard, R.L., Osborne, C.A., Firestone, M.K., 2013. Responses of soil bacterial and fungal communities to extreme desiccation and rewetting. ISME J. 7, 2229–2241.

Bartoń, K., 2020. MuMIn: Multi-Model Inference.

Bates, D., Mächler, M., Bolker, B., Walker, S., 2015. Fitting Linear Mixed-Effects Models Using lme4. J. Stat. Softw. 67.

Battaglia, T., 2020. btools: A suite of R function for all types of microbial diversity analyses. R package version 0.0.1.

Billings, S.A., Sullivan, P.L., Souza, L., Loecke, T.D., Hauser, E., Lang, K., Charles, R., Hirmas, D., Richter, D.D., Cherkinsky, A., Markewitz, D., 2019. Anthropogenic Declines in Deep Roots Constrain Deep Soil Organic Carbon Forms and Fluxes.

Bissett, A., Richardson, A.E., Baker, G., Thrall, P.H., 2011. Long-term land use effects on soil microbial community structure and function. Appl. Soil Ecol. 51, 66–78.

Bolyen, E., Rideout, J.R., Dillon, M.R., Bokulich, N.A., Abnet, C.C., Al-Ghalith, G.A., Alexander, H., Alm, E.J., Arumugam, M., Asnicar, F., Bai, Y., Bisanz, J.E., Bittinger, K., Brejnrod, A., Brislawn, C.J., Brown, C.T., Callahan, B.J., Caraballo-Rodríguez, A.M., Chase, J., Cope, E.K., Da Silva, R., Diener, C., Dorrestein, P.C., Douglas, G.M., Durall, D.M., Duvallet, C., Edwardson, C.F., Ernst, M., Estaki, M., Fouquier, J., Gauglitz, J.M., Gibbons, S.M., Gibson, D.L., Gonzalez, A., Gorlick, K., Guo, J., Hillmann, B., Holmes, S., Holste, H., Huttenhower, C., Huttley, G.A., Janssen, S., Jarmusch, A.K., Jiang, L., Kaehler, B.D., Kang, K.B., Keefe, C.R., Keim, P., Kelley, S.T., Knights, D., Koester, I., Kosciolek, T., Kreps, J., Langille, M.G.I., Lee, J., Ley, R., Liu, Y.-X., Loftfield, E., Lozupone, C., Maher, M., Marotz, C., Martin, B.D., McDonald, D., McIver, L.J., Melnik, A.V., Metcalf, J.L., Morgan, S.C., Morton, J.T., Naimey, A.T., Navas-Molina, J.A., Nothias, L.F., Orchanian, S.B., Pearson, T., Peoples, S.L., Petras, D., Preuss, M.L., Pruesse, E., Rasmussen, L.B., Rivers, A., Robeson, M.S., Rosenthal, P., Segata, N., Shaffer, M., Shiffer, A., Sinha, R., Song, S.J., Spear, J.R., Swafford, A.D., Thompson, L.R., Torres, P.J., Trinh, P., Tripathi, A., Turnbaugh, P.J., Ul-Hasan, S., vander Hooft, J.J.J., Vargas, F., Vázquez-Baeza, Y., Vogtmann, E., von Hippel, M., Walters, W., Wan, Y., Wang, M., Warren, J., Weber, K.C., Williamson, C.H.D., Willis, A.D., Xu, Z.Z., Zaneveld, J.R., Zhang, Y., Zhu, Q., Knight, R., Caporaso, J.G., 2019. Reproducible, interactive, scalable and extensible microbiome data science using QIIME 2. Nat. Biotechnol. 37, 852–857.

Brinkmann, N., Schneider, D., Sahner, J., Ballauff, J., Edy, N., Barus, H., Irawan, B., Budi, S.W., Qaim, M., Daniel, R., Polle, A., 2019. Intensive tropical land use massively shifts soil fungal communities. Sci. Rep. 9, 1–11.

Broeckling, C.D., Broz, A.K., Bergelson, J., Manter, D.K., Vivanco, J.M., 2008. Root Exudates Regulate Soil Fungal Community Composition and Diversity. Appl. Environ. Microbiol. 74, 738–744.

Callahan, B.J., McMurdie, P.J., Rosen, M.J., Han, A.W., Johnson, A.J.A., Holmes, S.P., 2016. DADA2: High resolution sample inference from Illumina amplicon data. Nat. Methods 13, 581–583.

Canarini, A., Kaiser, C., Merchant, A., Richter, A., Wanek, W., 2019. Root Exudation of Primary Metabolites: Mechanisms and Their Roles in Plant Responses to Environmental Stimuli. Front. Plant Sci. 10.

Caruso, V., Song, X., Asquith, M., Karstens, L., 2019. Performance of Microbiome Sequence Inference Methods in Environments with Varying Biomass. mSystems 4.

Cruz-Martínez, K., Suttle, K.B., Brodie, E.L., Power, M.E., Andersen, G.L., Banfield, J.F., 2009. Despite strong seasonal responses, soil microbial consortia are more resilient to long-term changes in rainfall than overlying grassland. ISME J. 3, 738–744.

de Vries, F.T., Griffiths, R.I., Bailey, M., Craig, H., Girlanda, M., Gweon, H.S., Hallin, S., Kaisermann, A., Keith, A.M., Kretzschmar, M., Lemanceau, P., Lumini, E., Mason, K.E., Oliver, A., Ostle, N., Prosser, J.I., Thion, C., Thomson, B., Bardgett, R.D., 2018. Soil bacterial networks are less stable under drought than fungal networks. Nat. Commun. 9.

Delgado□Baquerizo, M., Maestre, F.T., Reich, P.B., Trivedi, P., Osanai, Y., Liu, Y.-R., Hamonts, K., Jeffries, T.C., Singh, B.K., 2016. Carbon content and climate variability drive global soil bacterial diversity patterns. Ecol. Monogr. 86, 373–390.

Eilers, K.G., Debenport, S., Anderson, S., Fierer, N., 2012. Digging deeper to find unique microbial communities: The strong effect of depth on the structure of bacterial and archaeal communities in soil. Soil Biol. Biochem. 50, 58–65.

Evans, S.E., Wallenstein, M.D., 2012. Soil microbial community response to drying and rewetting stress: does historical precipitation regime matter? Biogeochemistry 109, 101–116.

Feng, H., Guo, J., Wang, W., Song, X., Yu, S., 2019. Soil Depth Determines the Composition and Diversity of Bacterial and Archaeal Communities in a Poplar Plantation. Forests 10, 550.

Fierer, N., Jackson, R.B., 2006. The diversity and biogeography of soil bacterial communities. Proc. Natl. Acad. Sci. 103, 626–631.

Fierer, N., Schimel, J.P., Holden, P.A., 2003. Variations in microbial community composition through two soil depth profiles. Soil Biol. Biochem. 35, 167–176.

Ge, G., Li, Z., Fan, F., Chu, G., Hou, Z., Liang, Y., 2009. Soil biological activity and their seasonal variations in response to long-term application of organic and inorganic fertilizers. Plant Soil 326, 31.

Glassman, S.I., Martiny, J.B.H., 2018. Broadscale Ecological Patterns Are Robust to Use of Exact Sequence Variants versus Operational Taxonomic Units. mSphere 3, e00148-18.

Glassman, S.I., Wang, I.J., Bruns, T.D., 2017. Environmental filtering by pH and soil nutrients drives community assembly in fungi at fine spatial scales. Mol. Ecol. 26, 6960–6973.

Griffiths, R.I., Whiteley, A.S., O'Donnell, A.G., Bailey, M.J., 2003. Influence of depth and sampling time on bacterial community structure in an upland grassland soil. FEMS Microbiol. Ecol. 43, 35–43.

Habekost, M., Eisenhauer, N., Scheu, S., Steinbeiss, S., Weigelt, A., Gleixner, G., 2008. Seasonal changes in the soil microbial community in a grassland plant diversity gradient four years after establishment. Soil Biol. Biochem. 40, 2588–2595.

Hamel, C., Hanson, K., Selles, F., Cruz, A.F., Lemke, R., McConkey, B., Zentner, R., 2006. Seasonal and long-term resource-related variations in soil microbial communities in wheat-based rotations of the Canadian prairie. Soil Biol. Biochem. 38, 2104–2116.

Hao, J., Chai, Y.N., Ordóñez, R.A., Wright, E.E., Archontoulis, S., Schachtman, D.P., 2020. The effects of soil depth on the structure of microbial communities in agricultural soils in Iowa, USA. bioRxiv 2020.03.31.018416.

Hartmann, M., Lee, S., Hallam, S.J., Mohn, W.W., 2009. Bacterial, archaeal and eukaryal community structures throughout soil horizons of harvested and naturally disturbed forest stands. Environ. Microbiol. 11, 3045–3062.

Hatfield, J.L., Sauer, T.J., Cruse, R.M., 2017. Chapter One - Soil: The Forgotten Piece of the Water, Food, Energy Nexus, in: Sparks, D.L. (Ed.), Advances in Agronomy. Academic Press, pp. 1–46.

Hawkes, C.V., Keitt, T.H., 2015. Resilience vs. historical contingency in microbial responses to environmental change. Ecol. Lett. 18, 612–625.

Hawkes, C.V., Kivlin, S.N., Rocca, J.D., Huguet, V., Thomsen, M.A., Suttle, K.B., 2011. Fungal community responses to precipitation. Glob. Change Biol. 17, 1637–1645.

Hawkes, C.V., Waring, B.G., Rocca, J.D., Kivlin, S.N., 2017. Historical climate controls soil respiration responses to current soil moisture. Proc. Natl. Acad. Sci. 114, 6322–6327.

Hurlbert, S.H., 1984. Pseudoreplication and the Design of Ecological Field Experiments. Ecol. Monogr. 54, 187–211.

Ihrmark, K., Bödeker, I.T.M., Cruz□Martinez, K., Friberg, H., Kubartova, A., Schenck, J., Strid, Y., Stenlid, J., Brandström□Durling, M., Clemmensen, K.E., Lindahl, B.D., 2012. New primers to amplify the fungal ITS2 region – evaluation by 454-sequencing of artificial and natural communities. FEMS Microbiol. Ecol. 82, 666–677.

Jangid, K., Williams, M.A., Franzluebbers, A.J., Schmidt, T.M., Coleman, D.C., Whitman, W.B., 2011. Land-use history has a stronger impact on soil microbial community composition than aboveground vegetation and soil properties. Soil Biol. Biochem. 43, 2184–2193.

Jobbágy, E.G., Jackson, R.B., 2001. The distribution of soil nutrients with depth: Global patterns and the imprint of plants. Biogeochemistry 53, 51–77.

Jumpponen, A., Jones, K.L., Blair, J., 2010. Vertical distribution of fungal communities in tallgrass prairie soil. Mycologia 102, 1027–1041.

Kang, S., Mills, A.L., 2006. The effect of sample size in studies of soil microbial community structure. J. Microbiol. Methods 66, 242–250.

Kurc, S.A., Small, E.E., 2007. Soil moisture variations and ecosystem-scale fluxes of water and carbon in semiarid grassland and shrubland. Water Resour. Res. 43.

Kuznetsova, A., Brockhoff, P.B., Christensen, R.H.B., 2017. lmerTest Package: Tests in Linear Mixed Effects Models. J. Stat. Softw. 82.

Lauber, C.L., Ramirez, K.S., Aanderud, Z., Lennon, J., Fierer, N., 2013. Temporal variability in soil microbial communities across land-use types. ISME J. 7, 1641–1650.

Lenth, R., Singmann, H., Love, J., Buerkner, P., Herve, M., 2020. emmeans: Estimated Marginal Means, aka Least-Squares Means.

Litchman, E., Edwards, K.F., Klausmeier, C.A., 2015. Microbial resource utilization traits and trade-offs: implications for community structure, functioning, and biogeochemical impacts at present and in the future. Front. Microbiol. 6.

McKenna, T.P., Crews, T.E., Kemp, L., Sikes, B.A., 2020. Community structure of soil fungi in a novel perennial crop monoculture, annual agriculture, and native prairie reconstruction. PLOS ONE 15, e0228202.

McMurdie, P.J., Holmes, S., 2013. phyloseq: An R Package for Reproducible Interactive Analysis and Graphics of Microbiome Census Data. PLOS ONE 8, e61217.

Nilsson, R.H., Larsson, K.-H., Taylor, A.F.S., Bengtsson-Palme, J., Jeppesen, T.S., Schigel, D., Kennedy, P., Picard, K., Glöckner, F.O., Tedersoo, L., Saar, I., Kõljalg, U., Abarenkov, K., 2019. The UNITE database for molecular identification of fungi: handling dark taxa and parallel taxonomic classifications. Nucleic Acids Res. 47, D259–D264.

Osburn, E.D., McBride, S.G., Aylward, F.O., Badgley, B.D., Strahm, B.D., Knoepp, J.D., Barrett, J.E., 2019. Soil Bacterial and Fungal Communities Exhibit Distinct Long-Term Responses to Disturbance in Temperate Forests. Front. Microbiol. 10.

Parada, A.E., Needham, D.M., Fuhrman, J.A., 2016. Every base matters: assessing small subunit rRNA primers for marine microbiomes with mock communities, time series and global field samples. Environ. Microbiol. 18, 1403–1414.

Philippot, L., Spor, A., Hénault, C., Bru, D., Bizouard, F., Jones, C.M., Sarr, A., Maron, P.-A., 2013. Loss in microbial diversity affects nitrogen cycling in soil. ISME J. 7, 1609–1619.

Price, M.N., Dehal, P.S., Arkin, A.P., 2010. FastTree 2--approximately maximum-likelihood trees for large alignments. PloS One 5, e9490.

Quast, C., Pruesse, E., Yilmaz, P., Gerken, J., Schweer, T., Yarza, P., Peplies, J., Glöckner, F.O., 2013. The SILVA ribosomal RNA gene database project: improved data processing and web-based tools. Nucleic Acids Res. 41, D590–D596.

R Core Team, 2019. R: A language and environment for statistical computing. R Foundation for Statistical Computing, Vienna, Austria.

Semenova□Nelsen, T.A., Platt, W.J., Patterson, T.R., Huffman, J., Sikes, B.A., 2019. Frequent fire reorganizes fungal communities and slows decomposition across a heterogeneous pine savanna landscape. New Phytol. 224, 916–927.

Shi, Y., Lalande, R., Hamel, C., Ziadi, N., Gagnon, B., Hu, Z., 2013. Seasonal variation of microbial biomass, activity, and community structure in soil under different tillage and phosphorus management practices. Biol. Fertil. Soils 49, 803–818.

Shigyo, N., Umeki, K., Hirao, T., 2019. Seasonal Dynamics of Soil Fungal and Bacterial Communities in Cool-Temperate Montane Forests. Front. Microbiol. 10.

Slessarev, E.W., Lin, Y., Bingham, N.L., Johnson, J.E., Dai, Y., Schimel, J.P., Chadwick, O.A., 2016. Water balance creates a threshold in soil pH at the global scale. Nature 540, 567–569.

Smith, A.P., Marín-Spiotta, E., de Graaff, M.A., Balser, T.C., 2014. Microbial community structure varies across soil organic matter aggregate pools during tropical land cover change. Soil Biol. Biochem. 77, 292–303.

Song, Z., Schlatter, D., Kennedy, P., Kinkel, L.L., Kistler, H.C., Nguyen, N., Bates, S.T., 2015. Effort versus Reward: Preparing Samples for Fungal Community Characterization in High-Throughput Sequencing Surveys of Soils. PLOS ONE 10, e0127234.

Steenwerth, K.L., Jackson, L.E., Calderón, F.J., Stromberg, M.R., Scow, K.M., 2002. Soil microbial community composition and land use history in cultivated and grassland ecosystems of coastal California. Soil Biol. Biochem. 34, 1599–1611.

Strickland, M.S., Lauber, C., Fierer, N., Bradford, M.A., 2009. Testing the functional significance of microbial community composition. Ecology 90, 441–451.

Thompson, L.R., Sanders, J.G., McDonald, D., Amir, A., Ladau, J., Locey, K.J., Prill, R.J., Tripathi, A., Gibbons, S.M., Ackermann, G., Navas-Molina, J.A., Janssen, S., Kopylova, E., Vázquez-Baeza, Y., González, A., Morton, J.T., Mirarab, S., Zech Xu, Z., Jiang, L., Haroon, M.F., Kanbar, J., Zhu, Q., Jin Song, S., Kosciolek, T., Bokulich, N.A., Lefler, J., Brislawn, C.J., Humphrey, G., Owens, S.M., Hampton-Marcell, J., Berg-Lyons, D., McKenzie, V., Fierer, N., Fuhrman, J.A., Clauset, A., Stevens, R.L., Shade, A., Pollard, K.S., Goodwin, K.D., Jansson, J.K., Gilbert, J.A., Knight, R., 2017. A communal catalogue reveals Earth's multiscale microbial diversity. Nature 551, 457–463.

Turley, N.E., Bell□Dereske, L., Evans, S.E., Brudvig, L.A., n.d. Agricultural land-use history and restoration impact soil microbial biodiversity. J. Appl. Ecol.

Veenstra, J.J., Lee Burras, C., 2015. Soil Profile Transformation after 50 Years of Agricultural Land Use. Soil Sci. Soc. Am. J. 79, 1154–1162.

Wang, X., Van Nostrand, J.D., Deng, Y., Lü, X., Wang, C., Zhou, J., Han, X., 2015. Scale-dependent effects of climate and geographic distance on bacterial diversity patterns across northern China's grasslands. FEMS Microbiol. Ecol. 91.

Waring, B., Hawkes, C.V., 2018. Ecological mechanisms underlying soil bacterial responses to rainfall along a steep natural precipitation gradient. FEMS Microbiol. Ecol. 94.

Weiler, M., Naef, F., 2003. An experimental tracer study of the role of macropores in infiltration in grassland soils. Hydrol. Process. 17, 477–493.

White, R.G., Kirkegaard, J.A., 2010. The distribution and abundance of wheat roots in a dense, structured subsoil--implications for water uptake. Plant Cell Environ. 33, 133–148.

White, T.J., Bruns, T., Lee, S., Taylor, J., 1990. Amplification and direct sequencing of fungal ribosomal RNA for phylogenetics, in: PCR Protocols. Elsevier, pp. 315–322.

Will, C., Thürmer, A., Wollherr, A., Nacke, H., Herold, N., Schrumpf, M., Gutknecht, J., Wubet, T., Buscot, F., Daniel, R., 2010. Horizon-Specific Bacterial Community Composition of German Grassland Soils, as Revealed by Pyrosequencing-Based Analysis of 16S rRNA Genes. Appl. Environ. Microbiol. 76, 6751–6759.

Williams, A., Vries, F.T. de, 2020. Plant root exudation under drought: implications for ecosystem functioning. New Phytol. 225, 1899–1905.

Xiang, D., Verbruggen, E., Hu, Y., Veresoglou, S.D., Rillig, M.C., Zhou, W., Xu, T., Li, H., Hao, Z., Chen, Y., Chen, B., 2014. Land use influences arbuscular mycorrhizal fungal communities in the farming–pastoral ecotone of northern China. New Phytol. 204, 968–978.

6 Supplementary Information

6.1 Supplementary Tables and Figures

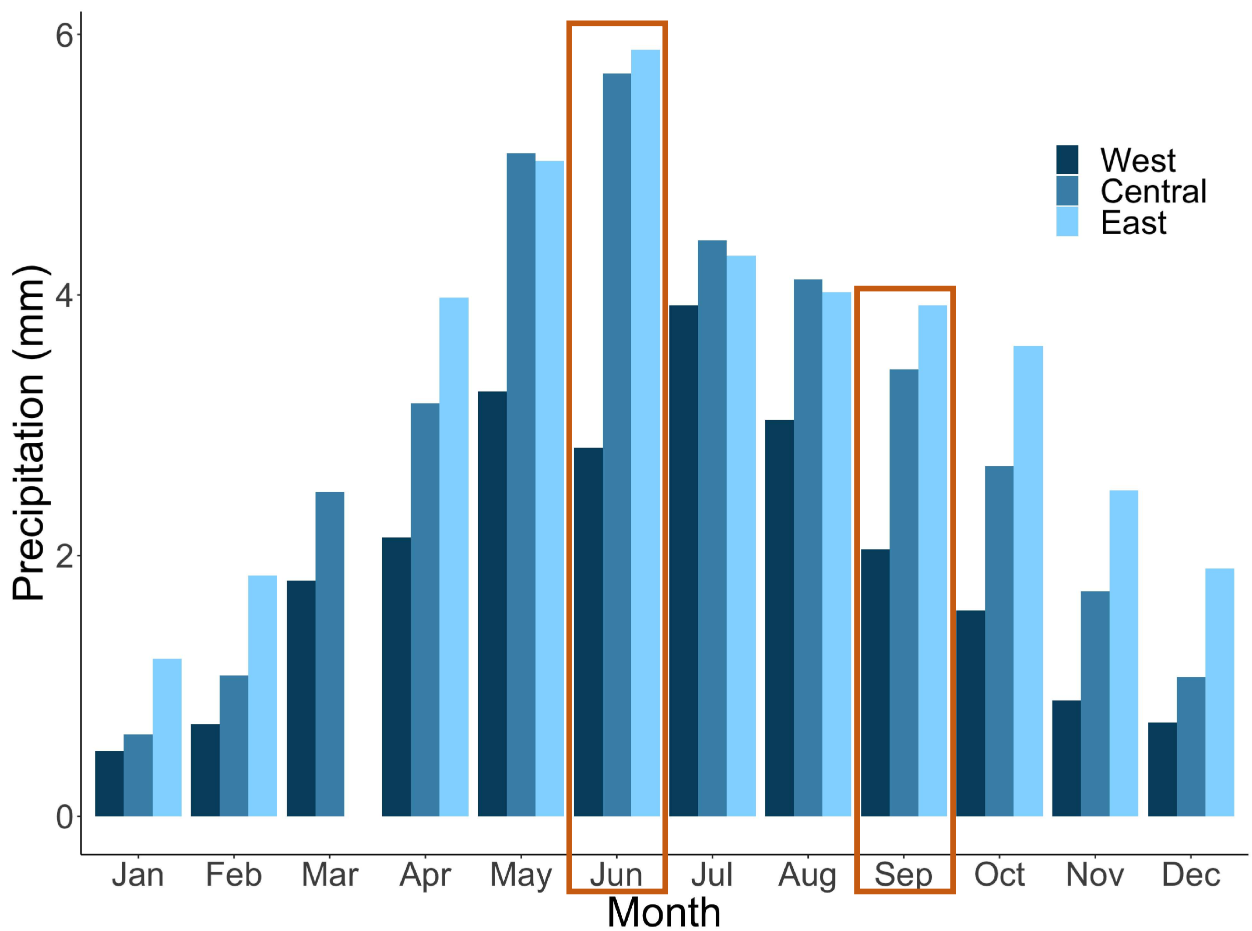

Supplementary Figure 1. Monthly average precipitation for each sampled region. Months are represented along the x-axis, and monthly precipitation in mm is represented along the y-axis. Colors represent West, Central, and East precipitation regions. Months in which samples were taken are highlighted in orange.

Supplementary Table 1 Post-hoc pairwise comparisons with Tukey-corrected *P* values for within-season bacterial diversity, measured using Faith's PD.

	Spring			Fall		
Contrast	**Estimate**	**Standard error**	***P* value**	**Estimate**	**Standard error**	***P* value**
5-15 — 15-30	1.836	0.677	$t_{111}=2.711$ $P=0.0587$	0.995	0.757	$t_{111}=1.314$ $P=0.683$
5-15 — 0-5	-0.713	0.675	$t_{110}=-1.056$ $P=0.8283$	1.676	0.761	$t_{113}=2.204$ $P=0.1859$
5-15 — 30-75	2.948	0.688	$t_{112}=4.282$ **$P=0.0004$ *** **	1.939	0.755	$t_{111}=2.567$ $P=0.0836$
5-15 — 75+	3.479	0.757	$t_{115}=4.595$ **$P=0.0001$ *** **	4.887	0.852	$t_{113}=5.733$ **$P<0.0001$ *** **
15-30 — 0-5	-2.549	0.705	$t_{112}=-3.614$ **$P=0.0041$ ** **	0.681	0.780	$t_{115}=0.874$ $P=0.9060$
15-30 — 30-75	1.112	0.671	$t_{111}=1.658$ $P=0.4644$	0.944	0.756	$t_{110}=1.248$ $P=0.7231$
15-30 — 75+	1.643	0.774	$t_{116}=2.122$ $P=0.2176$	3.892	0.856	$t_{113}=4.547$ **$P=0.0001$ *** **
0-5 — 30-75	3.661	0.715	$t_{113}=5.118$ **$P<0.0001$ *** **	0.263	0.785	$t_{116}=0.335$ $P=0.9973$
0-5 — 75+	4.192	0.756	$t_{113}=5.546$ **$P<0.0001$ *** **	3.211	0.870	$t_{116}=3.691$ **$P=0.0031$ ** **
30-75 — 75+	0.531	0.784	$t_{117}=0.677$ $P=0.9611$	2.948	0.855	$t_{113}=3.447$ **$P=0.0070$ ** **

Supplementary Table 2 Post-hoc pairwise comparisons with Tukey-corrected *P* values for fungal diversity, measured using Inverse Simpson.

	Spring			Fall		
Contrast	**Estimate**	**Standard error**	***P* value**	**Estimate**	**Standard error**	***P* value**
Soil depth						
5-15 — 15-30	0.955	5.62	$t_{142}=0.170$ $P=0.9998$	4.785	4.08	$t_{141}=1.173$ $P=0.7669$
5-15 — 0-5	-2.777	5.59	$t_{142}=-0.497$ $P=0.9876$	-6.222	3.99	$t_{141}=-1.559$ $P=0.5260$
5-15 — 30-75	-14.357	5.59	$t_{142}=-2.568$ $P=0.0820$	0.896	4.14	$t_{141}=0.217$ $P=0.9995$
5-15 — 75+	-32.040	6.01	$t_{142}=-5.330$ **P<0.0001 *** **	-12.343	4.89	$t_{141}=-2.526$ $P=0.0906$
15-30 — 0-5	-3.732	5.57	$t_{142}=-0.670$ $P=0.9626$	-11.007	4.07	$t_{141}=-2.707$ $P=0.0579$
15-30 — 30-75	-15.312	5.56	$t_{142}=-2.752$ $P=0.0516$	-3.889	4.06	$t_{141}=-0.959$ $P=0.0579$
15-30 — 75+	-32.996	5.88	$t_{142}=-5.608$ **$P<0.0001$ *** **	-17.128	4.64	$t_{141}=-3.694$ **$P=0.0029$ ** **
0-5 — 30-75	-11.580	5.54	$t_{142}=-2.090$ $P=0.2303$	7.118	4.12	$t_{141}=1.726$ $P=0.4215$
0-5 — 75+	-29.263	5.96	$t_{142}=-4.911$ **$P<0.0001$ *** **	-6.120	4.86	$t_{141}=-1.259$ $P=0.7163$
30-75 — 75+	-17.684	5.95	$t_{142}=-2.974$ **$P=0.0281$ * **	-13.239	4.68	$t_{141}=-2.827$ **$P=0.0422$ * **

Region						
East — West	11.64	4.39	t_{142}=2.649 ***P*=0.0243 ***	4.64	3.51	t_{141}=1.320 *P*=0.3862
East — Central	17.18	4.42	t_{142}=3.891 ***P*=0.0004 *****	13.78	3.33	t_{141}=4.138 ***P*=0.0002 *****
West — Central	-17.684	4.44	t_{142}=1.248 *P*=0.4272	9.14	3.24	t_{141}=2.818 ***P*=0.0152 ***
Depth x region *Significant contrasts only. W=West, C=Central, E=East						
E 5-15 — E 30-75	-38.274	9.70	t_{142}=-3.945 ***P*=0.0102 ***	—	—	—
E 5-15 — E 75+	-48.412	10.01	t_{142}=-4.837 ***P*=0.0003 *****	-36.787	9.03	t_{141}=-4.074 ***P*=0.0065 ****
E 5-15 — W 75+	-37.355	10.27	t_{142}=-3.638 ***P*=0.0283 ***	—	—	—
E 15-30 — E 30-75	-37.664	9.79	t_{142}=-3.848 ***P*=0.0143 ***	—	—	—
E 15-30 — E 75+	-47.801	10.08	t_{142}=-4.742 ***P*=0.0005 *****	-41.082	8.81	t_{141}=-4.661 ***P*=0.0007 *****
E 15-30 — W 75+	-36.744	10.29	t_{142}=-3.572 ***P*=0.0349 ***	—	—	—
E 0-5 — E 75+	-39.737	10.00	t_{142}=-3.972 ***P*=0.0093 ****	—	—	—
E 30-75 — E 75+	—	—	—	-33.555	8.72	t_{141}=-3.850 ***P*=0.0142 ***
E 30-75 — W 5-15	38.085	9.67	t_{142}=3.937 ***P*=0.0105 ***	—	—	—
E 30-75 — W 15-30	36.747	9.69	t_{142}=23.793 ***P*=0.0171 ***	—	—	—
E 30-75 — W 0-5	42.197	9.67	t_{142}=4.363 ***P*=0.0022 ****	—	—	—
E 30-75 — W 30-75	35.638	9.68	t_{142}=3.682 ***P*=0.0246 ***	—	—	—
E 30-75 — C 5-15	38.630	10.14	t_{142}=3.809 ***P*=0.0162 ***	—	—	—
E 30-75 — C 15-30	43.444	9.89	t_{142}=4.391 ***P*=0.0020 ****	—	—	—
E 30-75 — C 0-5	34.862	9.90	t_{142}=3.523 ***P*=0.0405 ***	—	—	—
E 30-75 — C 30-75	36.281	9.72	t_{142}=3.732 ***P*=0.0209 ***	—	—	—
E 75+ — W 5-15	48.223	10.00	t_{142}=4.822 ***P*=0.0003 *****	35.491	9.04	t_{141}=3.926 ***P*=0.0109 ***
E 75+ — W 15-30	46.885	10.00	t_{142}=4.689 ***P*=0.0006 *****	38.126	8.86	t_{141}=4.303 ***P*=0.0028 ****
E 75+ — W 0-5	52.335	9.99	t_{142}=5.237 ***P*=0.0001 *****	33.264	8.98	t_{141}=3.706 ***P*=0.0228 ***
E 75+ — W 30-75	45.776	10.01	t_{142}=4.575 ***P*=0.0010 ****	—	—	—
E 75+ — C 5-15	48.768	10.45	t_{142}=4.666 ***P*=0.0007 *****	37.793	8.86	t_{141}=4.268 ***P*=0.0032 ****
E 75+ — C 15-30	53.582	10.21	t_{142}=5.250 ***P*=0.0001 *****	45.217	8.59	t_{141}=5.265 ***P*=0.0001 *****
E 75+ — C 0-5	45.000	10.22	t_{142}=4.405 ***P*=0.0019 ****	—	—	—
E 75+ — C 30-75	46.419	10.02	t_{142}=4.631 ***P*=0.0008 *****	49.272	8.73	t_{141}=5.646 ***P*<0.0001 *****
E 75+ — C 75+	38.224	10.68	t_{142}=3.580 ***P*=0.0339 ***	46.797	9.13	t_{141}=5.127 ***P*=0.0001 *****
W 5-15 — W 75+	-37.166	10.32	t_{142}=-3.601 ***P*=0.0319 ***	—	—	—

W 15-30 — W 75+	-35.828	10.27	t_{142}=-3.488 ***P*=0.0449 ***	—	—	—
W 0-5 — W 75+	-41.278	10.30	t_{142}=-4.008 ***P*=0.0082 ****	—	—	—
W 75+ — C 5-15	37.711	10.76	t_{142}=3.504 ***P*=0.0428 ***	—	—	—
W 75+ — C 30-75	42.525	10.50	t_{142}=4.050 ***P*=0.0071 ****	—	—	—

Supplementary Table 3. Calculations for total amounts of variation in bacterial community structure in the spring.

Axis	**Variation explained by axis**	**GLMM mR^2**	**Model variation explained by fixed predictors**					**Community variation explained by fixed predictors by axis**				
	Axis relative eigenvalue		ANOVA SS/SS_{total}					Axis eig * GLMM R^2 * ANOVA SS/SS_{total}				
			Depth	**Region**	**Depth x region**	**Land use**	**Depth x land use**	**Depth**	**Region**	**Depth x region**	**Land use**	**Depth x land use**
1	0.1419	0.8279	0.7086	0.0488	0.2197	0.0021	0.0208	0.0832	0.0057	0.0258	0.0002	0.0024
2	0.0992	0.8698	0.9134	0.0309	0.0214	0.0026	0.0317	0.0788	0.0027	0.0018	0.0002	0.0027
3	0.0801	0.7223	0.4071	0.0140	0.5410	0.0009	0.0369	0.0236	0.0008	0.0313	0.0001	0.0021
4	0.0524	0.5985	0.5954	0.0288	0.2285	0.0259	0.1214	0.0187	0.0009	0.0072	0.0008	0.0038
5	0.0346	0.7338	0.0674	0.1513	0.7179	0.0085	0.0549	0.0017	0.0038	0.0182	0.0002	0.0014
6	0.0333	0.2200	0.0854	0.0696	0.3170	0.0175	0.5105	0.0006	0.0005	0.0023	0.0001	0.0037
7	0.0293	0.5888	0.0784	0.0176	0.8636	0.0016	0.0387	0.0014	0.0003	0.0149	0.0000	0.0007
8	0.0280	0.6343	0.3404	0.0012	0.2226	0.0361	0.3997	0.0060	0.0000	0.0040	0.0006	0.0071
9	0.0219	0.2280	0.2710	0.0273	0.2964	0.0110	0.3943	0.0014	0.0001	0.0015	0.0001	0.0020
							Sum:	0.2153	0.0149	0.1070	0.0024	0.0260

Total community variation explained by fixed predictors

Supplementary Table 4. Calculations for total amounts of variation in bacterial community structure in the fall.

Axis	**Variation explained by axis**	**GLMM mR^2**	**Model variation explained by fixed predictors**					**Community variation explained by fixed predictors by axis**				
	Axis relative eigenvalue		ANOVA SS/SS_{total}					Axis eig * GLMM R^2 * ANOVA SS/SS_{total}				
			Depth	**Region**	**Depth x region**	**Land use**	**Depth x land use**	**Depth**	**Region**	**Depth x region**	**Land use**	**Depth x land use**
1	0.1135	0.7345	0.7888	0.0219	0.1704	0.0002	0.0187	0.0658	0.0018	0.0142	0.0000	0.0016
2	0.0959	0.6874	0.8874	0.0209	0.0492	0.0073	0.0353	0.0585	0.0014	0.0032	0.0005	0.0023
3	0.0748	0.6682	0.4707	0.0160	0.3071	0.0062	0.2000	0.0235	0.0008	0.0153	0.0003	0.0100
4	0.0601	0.6237	0.5533	0.0181	0.2728	0.0159	0.1399	0.0207	0.0007	0.0102	0.0006	0.0052
5	0.0377	0.5402	0.1029	0.0135	0.7208	0.0001	0.1628	0.0021	0.0002	0.0147	0.0000	0.0033
6	0.0342	0.3013	0.2468	0.0080	0.6781	0.0078	0.0594	0.0025	0.0001	0.0070	0.0001	0.0006
7	0.0297	0.4935	0.2930	0.0077	0.3465	0.0030	0.3498	0.0043	0.0001	0.0051	0.0000	0.0051
8	0.0253	0.7206	0.0566	0.0241	0.8039	0.0076	0.1078	0.0010	0.0004	0.0146	0.0001	0.0020
9	0.0205	0.2014	0.1616	0.0778	0.1548	0.0006	0.3997	0.0007	0.0003	0.0006	0.0000	0.0025
10	0.0196	0.2378	0.3572	0.0021	0.3549	0.0107	0.3943	0.0017	0.0000	0.0017	0.0000	0.0013
							Sum:	0.1808	0.0059	0.0867	0.0017	0.0339

Total community variation explained by fixed predictors

Supplementary Table 5. Calculations for total amounts of variation in fungal community structure in the spring.

Axis	**Variation explained by axis**	**GLMM mR^2**	**Model variation explained by fixed predictors**					**Community variation explained by fixed predictors by axis**				
	Axis relative eigenvalue		ANOVA SS/SS_{total}					Axis eig * GLMM R^2 * ANOVA SS/SS_{total}				
			Depth	**Region**	**Depth x region**	**Land use**	**Depth x land use**	**Depth**	**Region**	**Depth x region**	**Land use**	**Depth x land use**
1	0.1402	0.4970	0.3085	0.0420	0.4531	0.0422	0.1542	0.0215	0.0029	0.0316	0.0029	0.0107
2	0.1254	0.7103	0.4088	0.0384	0.2275	0.0689	0.2563	0.0364	0.0034	0.0203	0.0061	0.0228
3	0.1035	0.7232	0.8887	0.0006	0.0664	0.0074	0.0369	0.0665	0.0000	0.0050	0.0006	0.0028
4	0.0773	0.5472	0.2752	0.0365	0.3084	0.0031	0.3768	0.0101	0.0013	0.0114	0.0001	0.0139
5	0.0350	0.1565	0.3158	0.0002	0.2667	0.0037	0.4136	0.0017	0.0000	0.0015	0.0000	0.0023
6	0.0329	0.2949	0.2648	0.0522	0.5781	0.0005	0.1045	0.0026	0.0005	0.0056	0.0000	0.0010
							Sum:	0.1389	0.0082	0.0752	0.0098	0.0535
							Total community variation explained by fixed predictors					

Supplementary Table 6. Calculations for total amounts of variation in fungal community structure in the fall.

Axis	**Variation explained by axis**	**GLMM mR^2**	**Model variation explained by fixed predictors**					**Community variation explained by fixed predictors by axis**				
	Axis relative eigenvalue		ANOVA SS/SS_{total}					Axis eig * GLMM R^2 * ANOVA SS/SS_{total}				
			Depth	**Region**	**Depth x region**	**Land use**	**Depth x land use**	**Depth**	**Region**	**Depth x region**	**Land use**	**Depth x land use**
1	0.1497	0.7309	0.7946	0.0032	0.0186	0.0232	0.1605	0.0869	0.0003	0.0020	0.0025	0.176
2	0.1130	0.7368	0.7248	0.0440	0.1485	0.0036	0.0791	0.0603	0.0037	0.0124	0.0003	0.0066
3	0.0697	0.7608	0.7276	0.0095	0.0832	0.0119	0.1679	0.0386	0.0005	0.0044	0.0006	0.0089
4	0.0509	0.5781	0.7282	0.0518	0.1441	0.0042	0.0718	0.0214	0.0015	0.0042	0.0001	0.0021
5	0.0389	0.4050	0.3801	0.0179	0.1436	0.0051	0.4533	0.0060	0.0003	0.0023	0.0001	0.0071
6	0.0339	0.2459	0.0896	0.0079	0.5581	0.0035	0.3408	0.0007	0.0001	0.0047	0.0000	0.0028
7	0.0276	0.3375	0.4052	0.0344	0.2158	0.0433	0.3014	0.0038	0.0003	0.0020	0.0004	0.0028
8	0.0268	0.1862	0.0704	0.0013	0.8185	0.0020	0.1078	0.0004	0.0000	0.0041	0.0000	0.0005
							SUM:	0.2181	0.0067	0.0361	0.0041	0.0485
							Total community variation explained by fixed predictors					

Supplementary Table 7. Post-hoc pairwise comparisons with Tukey-corrected *P* values for magnitudes of seasonal change in bacterial diversity, measured using the difference between spring and fall Faith's PD.

Contrast	**Estimate**	**Standard error**	***P* value**
15-30 — 5-15	-0.278	0.680	t_{61}=-0.408 *P*=0.912
15-30 — 0-5	-1.796	0.681	t_{62}=-2.635 ***P*=0.0282 ***
5-15 — 0-5	-1.518	0.684	t_{62}=-2.22 *P*=0.0757

Supplementary Table 8. Post-hoc pairwise comparisons with Tukey-corrected *P* values for magnitudes of seasonal change in bacterial community structure, measured using distances between spring and fall Bray-Curtis dissimilarity indices.

Contrast	Estimate	Standard error	*P* value
Soil depth			
5-15 — 15-30	0.0138	0.0217	t_{62}=0.1639 *P*=0.7993
5-15 — 0-5	-0.1572	0.0216	t_{61}=-7.265 ***P*<0.0001** ***
15-30 — 0-5	-0.1711	0.0216	t_{61}=-7.902 ***P*<0.0001** ***
Depth x region *Significant contrasts only. W=West, C=Central, E=East			
W 5-15 — W 0-5	-0.24833	0.0369	t_{62}=-6.736 ***P*<0.0001** ***
C 5-15 — W 0-5	-0.41744	0.0879	t_{5}=-4.751 ***P*=0.0487** *
E 15-30 — E 0-5	-0.14023	0.0378	t_{61}=-3.713 ***P*=0.0124** *
W 15-30 — W 0-5	-0.28075	0.0371	t_{62}=-7.572 ***P*<0.0001** ***

Supplementary Table 9. Post-hoc pairwise comparisons with Tukey-corrected *P* values for magnitudes of seasonal change in fungal community structure, measured using distances between spring and fall Bray-Curtis dissimilarity indices.

Contrast	Estimate	Standard error	*P* value
Region			
East — West	0.0219	0.0336	t_{4}=0.654 *P*=0.8005
East — Central	0.1342	0.0338	t_{4}=3.969 ***P*=0.0343** *
West — Central	0.1122	0.0337	t_{4}=3.33 *P*=0.0608
Depth x region *Significant contrasts only. W=West, C=Central, E=East			
E 5-15 — C 15-30	0.21129	0.0436	t_{11}=4.846 ***P*=0.010** *
E 15-30 — C 15-30	0.2066	0.0444	t_{12}=4.655 ***P*=0.0117** *
W 15-30 — W 0-5	-0.13139	0.0329	t_{57}=-3.993 ***P*=0.0055** **
C 15-30 — E 0-5	-0.24114	0.0436	t_{11}=-5.53 ***P*=0.0037** **
W 0-5 — C 0-5	0.1935	0.0436	t_{11}=4.438 ***P*=0.0185** *

6.2 Bioinformatics pipelines

6.2.1 Bacteria

```
##### sequence processing in QIIME ------------------------
### import spring bacteria -------------------------------------
#!/bin/bash
#SBATCH --job-name=bact_imp                #Job name
#SBATCH --partition=sixhour                #Partition Name (required)
#SBATCH --ntasks=16                        #processors
#SBATCH --mem=350GB
#SBATCH --time=05:59:00                    #Time limit
#SBATCH --export=NONE
#SBATCH --output bact_imp2.log

module load qiime2
cd /home/p799h475/work/EPSCoR_bact_sp18/PH-EPSCOR-SB

qiime tools import \
--type 'SampleData[PairedEndSequencesWithQuality]' \
--input-path /home/p799h475/work/EPSCoR_bact_sp18/PH-EPSCOR-SB \
--input-format CasavaOneEightSingleLanePerSampleDirFmt \
--output-path demux-paired-end.qza

### import fall bacteria -----------------------------------------
#!/bin/bash
#SBATCH --job-name=bact_imp                #Job name
#SBATCH --partition=sixhour                #Partition Name (required)
#SBATCH --ntasks=16                        #processors
#SBATCH --mem=350GB
#SBATCH --time=05:59:00                    #Time limit
#SBATCH --export=NONE
#SBATCH --output bact_imp.log

module load qiime2/2019.7
cd /home/p799h475/work/EPSCoR_bact_sp18/PH-EPSCOR-SB

qiime tools import \
--type 'SampleData[PairedEndSequencesWithQuality]' \
--input-path /home/p799h475/work/EPSCoR_bact_fall18/PH-MAPS-Bacteria-F18-Sikes \
--input-format CasavaOneEightSingleLanePerSampleDirFmt \
--output-path demux-paired-end.qza
```

```
### dada2 denoise ---------------------------------------------
# spring ---------------------------------------------------------
#!/bin/bash
#SBATCH --job-name=bact_denoise          #Job name
#SBATCH --partition=sixhour              #Partition Name (required)
#SBATCH --ntasks=40                      #processors
#SBATCH --mem=50GB
#SBATCH --time=05:59:00                  #Time limit
#SBATCH --export=NONE
#SBATCH --output bact_denoise.log

module load qiime2
cd /home/p799h475/EPSCoR/EPSCoR_bact_sp18/PH-EPSCOR-SB

qiime dada2 denoise-paired \
--i-demultiplexed-seqs demux-paired-end.qza \
--p-trim-left-f 13  \
--p-trim-left-r 13 \
--p-trunc-len-f 270 \
--p-trunc-len-r 220 \
--o-table /home/p799h475/EPSCoR/EPSCoR_bact_sp18/working/table2.qza \
--o-representative-sequences /home/p799h475/EPSCoR/EPSCoR_bact_sp18/working/rep-seqs2.qza \
--o-denoising-stats /home/p799h475/EPSCoR/EPSCoR_bact_sp18/working/denoising-stats2.qza \
--p-n-threads 40

# fall -----------------------------------------------------------
#!/bin/bash
#SBATCH --job-name=bact_denoise          #Job name
#SBATCH --partition=sixhour              #Partition Name (required)
#SBATCH --ntasks=40                      #processors
#SBATCH --mem=50GB
#SBATCH --time=05:59:00                  #Time limit
#SBATCH --export=NONE
#SBATCH --output bact_denoise.log

module load qiime2
cd /home/p799h475/work/EPSCoR_bact_fall18/working

qiime dada2 denoise-paired \
--i-demultiplexed-seqs demux-paired-end.qza \
--p-trim-left-f 13 \
--p-trim-left-r 13 \
--p-trunc-len-f 270 \
--p-trunc-len-r 220 \
--o-table table.qza \
--o-representative-sequences rep-seqs.qza \
--o-denoising-stats denoising-stats.qza \
--p-n-threads 40
```

```
### merge spring and fall runs (tables and rep seqs) --------
qiime feature-table merge-seqs \
--i-data rep-seqs_new.qza \
--i-data rep-seqs2_sp.qza \
--o-merged-data rep-seqs_merged3.qza

qiime feature-table merge \
--i-tables id-filtered-table_bact_sp2.qza \
--i-tables table_new.qza \
--p-overlap-method sum \
--o-merged-table table_bact_merged3.qza

### create phylogenetic tree ------------------------------------
#!/bin/bash
#SBATCH --job-name=bact_tree              #Job name
#SBATCH --partition=sixhour               #Partition Name (required)
#SBATCH --ntasks=16                       #processors
#SBATCH --mem=350GB
#SBATCH --time=05:59:00                   #Time limit
#SBATCH --export=NONE
#SBATCH --output bact_tree.log

module load qiime2/2019.7
cd /home/p799h475/work/EPSCoR_bact

qiime phylogeny align-to-tree-mafft-fasttree \
--i-sequences rep-seqs_merged3.qza \
--o-alignment aligned-rep-seqs.qza \
--o-masked-alignment masked-aligned-rep-seqs.qza \
--o-tree unrooted-tree.qza \
--o-rooted-tree rooted-tree.qza

### output sequences, table, tree for phyloseq ----------------
qiime tools export \
--input-path rep-seqs_merged3.qza \
--output-path exported

qiime tools export \
--input-path rooted-tree.qza \
--output-path exported

qiime tools export \
--input-path table_bact_merged3.qza \
--output-path exported

biom convert \
-i feature-table.biom \
-o bact_merged_table2.txt \
--to-tsv
```

```
##### input to R -----------------------------------------------
library(genefilter)
library(phyloseq)
library(dada2)
library(Biostrings)
library(dplyr)
library(btools)

### import ASVs -----------------------------------------------
ASVs <- read.delim("bacteria_inputs_outputs/FINAL/bact_merged_table2.txt", header = TRUE,
        row.names = 1, check.names = FALSE)
ASVs <- otu_table(ASVs, taxa_are_rows = TRUE)

### import rep seqs -----------------------------------------------
repseqs <- readDNAStringSet("bacteria_inputs_outputs/bact_merged_sequences2.fasta")
repseqs <- getSequences(repseqs)

### assign taxonomy ---------------------------------------
taxa_bact <- assignTaxonomy(repseqs, silva_path, multithread = TRUE)
taxa_bact <- tax_table(taxa_bact)

### read in metadata ---------------------------------------
bact_metadata <- read.csv("bacteria_inputs_outputs/FINAL/EPSCoR_bact_merge_map.csv", header =
        TRUE, row.names = 1)
bact_metadata <- sample_data(bact_metadata)

### read in rooted tree --------------------------------------
bact_rooted <- read_tree('bacteria_inputs_outputs/rooted_tree.nwk')

### make phyloseq object -----------------------------------
bact_phylo <- phyloseq(ASVs, bact_metadata, taxa_bact, bact_rooted)

### additional quality filtering -----------------------------
# filtering out eukaryotes ------------------------------------
phylo_noeuk <- subset_taxa(bact_phylo, Kingdom %in% c('Archaea', 'Bacteria'))

# filtering out bad ASVs -----------------------------------
threshold <- kOverA(k=5, A=20)
phylo_thersholded <- filter_taxa(phylo_noeuk, threshold, prune = TRUE)

# filtering out failed samples -------------------------------
sum_phylo_thershold <- sample_sums(phylo_thersholded)
phylo_thresholded_highcover <- subset_samples(phylo_thersholded, sample_sums(phylo_thersholded) >
        1000)

### calculate faith's pd -------------------------------------
# spring -------------------------------------------------------
phylo_thresholded_alpha_sp <- subset_samples(phylo_thresholded_highcover, Season=='Spring')
sample_data(phylo_thresholded_alpha_sp)$UsableReads <- sample_sums(phylo_thresholded_alpha_sp)
sample_data(phylo_thresholded_alpha_sp)$Faith <- estimate_pd(phylo_thresholded_alpha_sp)
```

```
# fall --------------------------------------------------------
phylo_thresholded_alpha_fa <- subset_samples(phylo_thresholded_highcover, Season=='Fall')
sample_data(phylo_thresholded_alpha_fa)$UsableReads <- sample_sums(phylo_thresholded_alpha_fa)
sample_data(phylo_thresholded_alpha_fa)$Faith <- estimate_pd(phylo_thresholded_alpha_fa)
```

6.2.2 Fungi

```
##### sequence processing in QIIME ----------------------
### import spring fungi ---------------------------------------
#!/bin/bash
#SBATCH --job-name=fun_imp              #Job name
#SBATCH --partition=sixhour             #Partition Name (required)
#SBATCH --ntasks=16                     #processors
#SBATCH --mem=350GB
#SBATCH --time=05:59:00                         #Time limit
#SBATCH --export=NONE
#SBATCH --output fun_imp.log

module load qiime2
cd /home/p799h475/work/EPSCoR_fun_sp18/

qiime tools import \
 --type 'SampleData[PairedEndSequencesWithQuality]' \
 --input-path manifest_filepath \
 --output-path paired-end-demux.qza \
 --source-format PairedEndFastqManifestPhred33

### import fall fungi -------------------------------------------
#!/bin/bash
#SBATCH --job-name=Q2.imp               #Job name
#SBATCH --partition=sixhour             #Partition Name (required)
#SBATCH --ntasks=16                     #processors
#SBATCH --mem=350GB
#SBATCH --time=05:59:00                         #Time limit
#SBATCH --export=NONE
#SBATCH --output Q2.imp.log

module load qiime2
cd EPSCoR

qiime tools import \
--type 'SampleData[PairedEndSequencesWithQuality]' \
--input-path fungi_fall18_rawdata/ \
--input-format CasavaOneEightSingleLanePerSampleDirFmt \
--output-path demux-paired-end.qza
```

```
### dada2 denoise ---------------------------------------------
# spring ---------------------------------------------------------
#!/bin/bash
#SBATCH --job-name=denoise                  #Job name
#SBATCH --partition=sixhour                 #Partition Name (required)
#SBATCH --ntasks=40                         #processors
#SBATCH --mem=50GB
#SBATCH --time=05:59:00                             #Time limit
#SBATCH --export=NONE
#SBATCH --output fun_denoise.log

module load qiime2
cd /home/p799h475/work/EPSCoR_fun_sp18

qiime dada2 denoise-paired \
--i-demultiplexed-seqs paired-end-demux.qza \
--p-trim-left-f 13 \
--p-trim-left-r 13 \
--p-trunc-len-f 275 \
--p-trunc-len-r 220 \
--o-table table2.qza \
--o-representative-sequences rep-seqs2.qza \
--o-denoising-stats denoising-stats2.qza \
--p-n-threads 40

# fall -------------------------------------------------------------
#!/bin/bash
#SBATCH --job-name=denoise                  #Job name
#SBATCH --partition=sixhour                 #Partition Name (required)
#SBATCH --ntasks=40                         #processors
#SBATCH --mem=50GB
#SBATCH --time=05:59:00                             #Time limit
#SBATCH --export=NONE
#SBATCH --output denoise.log

module load qiime2
cd /home/p799h475/EPSCoR/EPSCoR_fun_fall18/fungi_fall18_15mar2020

qiime dada2 denoise-paired \
--i-demultiplexed-seqs demux-paired-end.qza \
--p-trim-left-f 13 \
--p-trim-left-r 13 \
--p-trunc-len-f 275 \
--p-trunc-len-r 220 \
--o-table table.qza \
--o-representative-sequences rep-seqs.qza \
--o-denoising-stats denoising-stats.qza \
--p-n-threads 40
```

```
# merge spring and fall runs (tables and rep seqs) ----------
qiime feature-table merge \
--i-tables fun_sp18_merge2/table2.qza \
--i-tables fun_fall18_merge2/table.qza \
--p-overlap-method sum \
--o-merged-table table_fungi_merged2.qza

qiime feature-table merge-seqs \
--i-data fun_sp18_merge2/rep-seqs2.qza \
--i-data fun_fall18_merge2/rep-seqs.qza \
--o-merged-data rep-seqs_fungi_merged2.qza

### creating OTUs ---------------------------------------------
# clean UNITE sequences ---------------------------------------
awk '/^>/ {print($0)}; /^[^>]/ {print(toupper($0))}' sh_refs_qiime_ver8_97_04.02.2020_dev.fasta | tr -d ' '
> sh_refs_qiime_ver8_97_04.02.2020_dev_uppercase.fasta

# import to QIIME -------------------------------------------
qiime tools import \
  --type 'FeatureData[Sequence]' \
  --input-path sh_refs_qiime_ver8_97_04.02.2020_dev_uppercase.fasta \
  --output-path 97_refs_otus_dev.qza

# create 97% OTUs -------------------------------------------
#!/bin/bash
#SBATCH --job-name=or_cluster            #Job name
#SBATCH --partition=sixhour              #Partition Name (required)
#SBATCH --ntasks=40                      #processors
#SBATCH --mem=50GB
#SBATCH --time=05:59:00                  #Time limit
#SBATCH --export=NONE
#SBATCH --output or_cluster_sp18.log

module load qiime2
cd /home/p799h475/work

qiime vsearch cluster-features-open-reference \
--i-table EPSCoR_fun_merge/table_fungi_merged2.qza \
--i-sequences EPSCoR_fun_merge/rep-seqs_fungi_merged2.qza \
--i-reference-sequences UNITE/developerUNITE/97_refs_otus_dev.qza \
--p-perc-identity 0.97 \
--o-clustered-table EPSCoR_fun_merge/table_fungi_merged_or_97dev.qza \
--o-clustered-sequences EPSCoR_fun_merge/rep-seqs_fungi_merged_or_97dev.qza \
--o-new-reference-sequences EPSCoR_fun_merge/new-ref-seqs_fungi_merged_97dev.qza

### output clustered sequences, table for phyloseq --------
qiime tools export \
--input-path table_fungi_merged_or_97dev.qza \
--output-path exported
```

```
biom convert \
-i exported/feature-table.biom \
-o exported/OTUtable_fungi_merged.txt \
--to-tsv

qiime tools export \
--input-path rep-seqs_fungi_merged_or_97dev.qza \
--output-path exported

##### input to R ------------------------------------------------
library(genefilter)
library(phyloseq)
library(dada2)
library(Biostrings)
library(dplyr)

### import OTUs ----------------------------------------------
OTUs <- read.delim("fungi_inputs_outputs/table_fungi_merged_orOTU_97dev_edit.txt", header =
        TRUE, row.names = 1, check.names = FALSE)
OTUs <- otu_table(OTUs, taxa_are_rows = TRUE)

### import rep seqs ---------------------------------------
f_repseqs <- readDNAStringSet("fungi_inputs_outputs/repseqs_fungi_merged_97dev.fasta")
f_repseqs <- getSequences(f_repseqs)

### assign taxonomy ---------------------------------------
taxa_fungi <- assignTaxonomy(f_repseqs, unite_path, multithread = TRUE)
taxa_fungi_table <- tax_table(taxa_fungi_mat)

### turn into phyloseq object ------------------------------
taxa_fungi_table <- tax_table(taxa_fungi_mat)

### read in metadata ---------------------------------------
fungi_metadata <- read.csv("fungi_inputs_outputs/fungi_metadata_merged.csv", header = TRUE,
        row.names = 1)
fungi_metadata <- sample_data(fungi_metadata)

### make phyloseq object --------------------------------
fungi_phylo <- phyloseq(OTUs, fungi_metadata, taxa_fungi_table)

### additional quality filtering --------------------------
# filtering out everything that is not fungi -------------
fungi_only_phylo <- subset_taxa(fungi_phylo, Kingdom %in% 'k__Fungi')

# filtering out bad OTUs ---------------------------------
threshold <- kOverA(k=5, A=20)
fungi_phylo_thersholded <- filter_taxa(fungi_only_phylo, threshold, prune = TRUE)
```

```
# filtering out failed samples ----------------------------
sum_fungi_phylo_thershold <- sample_sums(fungi_phylo_thersholded)
fungi_phylo_thresholded_highcover <- subset_samples(fungi_phylo_thersholded,
        sample_sums(fungi_phylo_thersholded) > 1000)

### calculate inverse simpson -----------------------------
# spring ------------------------------------------------------
f_thresholded_alpha_sp <- subset_samples(fungi_phylo_thersholded, Season=='Spring')
sample_data(f_thresholded_alpha_sp)$UsableReads <- sample_sums(f_thresholded_alpha_sp)
sample_data(f_thresholded_alpha_sp)$InvSimp <- estimate_richness(f_thresholded_alpha_sp,
        measures = 'InvSimpson')$InvSimp
# fall -----------------------------------------------------------
f_thresholded_alpha_fa <- subset_samples(fungi_phylo_thersholded, Season=='Fall')
sample_data(f_thresholded_alpha_fa)$UsableReads <- sample_sums(f_thresholded_alpha_fa)
sample_data(f_thresholded_alpha_fa)$InvSimp <- estimate_richness(f_thresholded_alpha_fa,
         measures = 'InvSimpson')$InvSimp
```